Original Article

Histological, Immunohistochemical, and Histomorphometric Studies on the Possible Curative Effect of Alendronic Acid (Fosamax), Vitamin K2 and / or Fennel on Ovariectomy-Induced Osteoporosis in Rats

Heba Yousef El-Yamany Aboudighied, Hekmat A. Ahmed Sorour and Mona Mohamed Abd-Elgalil Elsayed

Department of Histology and Cell Biology, Faculty of Medicine (Girls), Al-Azhar University, Cairo, Egypt

ABSTRACT

Aim of the Work: To evaluate the role of Alendronic acid (Fosamax), vitamin K2, and/or fennel essential oil in treating ovariectomy-induced osteoporosis in adult female albino rats.

Materials and Methods: Forty-eight adult female Wistar albino rats weighing 180±20g, aging 12-14 weeks were divided into the following groups: Group I (control group). Group II (sham-operated group), and group III (ovariectomized group). Bilateral ovariectomy (OVX) was performed for thirty rats and twelve weeks later, rats were further subdivided equally into five subgroups. Group IIIa (osteoporotic group); Group IIIb (Fosamax-treated group).Group IIIc (Mena Q- treated group); Group IIId (Fennel oil-treated group); Group IIIe (Mena Q and Fennel-treated group). All treatments were administered by oro-gastric tube and were continued for 12 weeks. Serum analysis was assessed for the appropriate laboratory tests. Femur bone specimens were processed for histological examination. Morphometric and statistical analyses were performed.

Results: The osteoporotic group showed a non-homogenous acidophilic matrix with osteoporotic cavities, large bony tunnels, areas devoid of osteocytes, empty lacunae, and unevenly eroded endosteum. These findings were supported by a significant decrease in serum calcium and phosphorus levels coupled with a significant increase in levels of the enzymes bone-specific alkaline phosphatase and tartrate-resistant acid phosphatase and a significant reduction in the area percentage of collagen fibers and Periodic-Acid-Schiff reaction within the bone matrix. The immunohistochemical studies detected a positive RANKL immune expression in the osteoporotic cavities and weak osteopontin expression within the bone matrix. Whereas, Fosamax, Vitamin K2, and fennel essential oil revealed obvious improvement in the histological changes depicted previously.

Conclusion: Combined administration of fennel essential oil and Vitamin K2 has a more pronounced enhancing healing effect in PMO than Vitamin K2, fennel separately, or Fosamax. This could be attributed to the synergistic antioxidant and anti-inflammatory properties in addition to the potent estrogenic effect of fennel.

Received: 22 July 2023, **Accepted:** 13 August 2023

Key Words: Fennel, fosamax, osteoporosis, ovariectomy, vitamin K2.

Corresponding Author: Heba Yousef El-Yamany Aboudighied, MSc, Department of Histology and Cell Biology, Faculty of Medicine (Girls), Al-Azhar University, Egypt, **Tel.** +2 010 2653 1286, **E-mail:** drhebayousefelyamany18@yahoo.com

ISSN: 1110-0559, Vol. 47, No. 3

INTRODUCTION

Low bone mass and microarchitectural deterioration of bone tissue are the hallmarks of osteoporosis, a systemic skeletal disease that raises the risk of fractures due to weakened bone strength[1]. Until a fracture occurs, it is a silent disease without evident symptoms or signs[2].

Menopause is the period in an adult woman's life when the ovaries gradually become inactive and menstruation ceases[3]. Following menopause, there is typically a dramatic decline in circulating estrogen levels, which results in accelerated bone resorption but not reformation and sets the stage for postmenopausal osteoporosis (PMO), a worldwide metabolic bone disorder affecting postmenopausal females. Age-related bone loss is caused by hormonal changes as well as decreased ability to utilize calcium, decreased vitamin D supply through lower synthesis and absorption, and decreased enzymatic hydroxylation of 25-hydroxycholecalciferol by the kidneys[4,5].

Following a bilateral oophorectomy, women experience surgical menopause since they lose most of their capability to produce estrogen and progesterone at substantial levels. The physiologic changes related to menopause in oophorectomy occur swiftly, with the more sudden and severe onset of symptoms having a major influence on a woman's well-being and quality of life[4].

DOI: 10.21608/ejh.2023.223198.1924

Alendronic acid promotes osteoblast differentiation and modifies the osteoclasts' capacity for bone resorption, which may contribute to bone remodeling in postmenopausal osteoporosis[5].

Vitamin K2 exerts a profound influence on bone building and has been listed as one of the most frequently prescribed therapies for osteoporosis and fracture[6].

Foeniculum Vulgare Mill (fennel) is one of the most widespread and well-known phytoestrogens due to its structural resemblance to diethylstilbestrol, a synthetic estrogen. Recently, phytoestrogens have received considerable interest as an implicit treatment for PMO, preventing cancer, and relieving menopausal symptoms[7,8].

The current work aimed to assess the role of Alendronic acid (Fosamax), vitamin K2, and fennel essential oil separately or in combination in ameliorating ovariectomized-induced osteoporosis in adult female albino rats.

MATERIALS AND METHODS

Animals, drugs, and chemicals

In the current study, 48 adult female Rattus norvogicus albino rats, aged 12–14 weeks and weighing 180 ± 20 g, were used. They had been purchased from the animal breeding farm, Helwan, Egypt. Rats were settled in standard-clean, adequately ventilated stainless steel mesh cages in a pathogen-free environment at the Faculty of Medicine for Girls, Al-Azhar University, Cairo, with a room temperature of 25 ±2˚C, a humidity of 54 ± 5%, and alternate light/dark cycles. Before the experiment began, rats were adapted for a week. During the experiment, rats had unrestricted access to food and water. According to the institutional animal care and use committee's (FMG-IRB) established ethical guidelines and procedures accepted by the Faculty of Medicine for Girls, Al Azhar University, all ethical protocols for treating animals were followed.

Fosamax (Alendronic acid), manufactured by Aecica Pharmaceuticals GmbH, Germany, was used. The 70 mg tablet was ground and dissolved in saline, then 1 ml of solution (0.2 mg/ml/rat) was administered orally once a week at an equivalent human dose of 70 mg/adult[9,10].

Mena Q: A highly purified long-acting form of vitamin K2 was used, manufactured by Dulexlab Devartlab Pharmaceuticals, Egypt. Each one-gram pill was ground and dissolved in saline, before being given orally once daily to rats (0.5 mg/ml/rat) at an equivalent human dose of 1 g/adult[11].

Fennel essential oil (Foeniculum vulgare Mill): Sigma-Aldrich Chemical Company (CAS Number 8006-84-6), St. Louis, Missouri, USA, was purchased from The Egyptian International Center for Import, Nasr City, Cairo, Egypt. 1 ml of fennel essential oil was given daily to the animals orally at an equivalent dose of 100 mg/kg body weight, according to the study of Kim *et al*.[12].

Experimental design

The rats were divided into three main groups:

Control group (GI, n = 12): that was further subdivided equally into two subgroups (6 animals each):

- Subgroup Ia: which served as a negative control, received no treatment.
- Subgroup Ib: included rats which received 1 ml of saline (a drug vehicle) orally once daily during the experimental period (24 weeks).

Sham-operated group (GII, n = 6): the ovaries were exteriorized but not removed, and then rats had unrestricted access to food and water with no treatment intervention during the entire experiment.

Ovariectomized group (GIII, n = 30): bilateral ovariectomy (OVX) was performed for thirty adult female albino rats according to Liu *et al*.[13]. The ovariectomized rats were then maintained for a further 12 weeks to induce osteoporosis, according to Liu *et al*.[13] and Rajfer *et al*.[14]. Rats from this cohort were further subdivided equally into five subgroups (6 animals each):

Osteoporotic group (Group IIIa): OVX rats were left without any treatment for another 12 weeks.

Fosamax-treated group (Group IIIb): OVX rats were given 1 ml of Fosamax solution (0.2 mg/ml/rat/week).

Mena Q-treated group (Group IIIc): OVX rats were administrated 1 ml of Mena Q solution once daily (0.5 mg/ml/rat).

Fennel-treated group (Group IIId): OVX rats received 1 ml of fennel essential oil daily at a dose equivalent to 100 mg/kg body weight.

Mena Q and Fennel-treated group (Group IIIe): OVX rats received Mena Q one hour prior to fennel in the same doses as groups IIIc and IIId, respectively.

All the treatments were introduced through an oro-gastric tube at 9:00 a.m. for 12 weeks following induced osteoporosis, and after that, rats were sacrificed.

Animals of all groups were weighted separately at the beginning and end of the experiment prior to sample collection.

By the end of the experiment, blood was collected from the retro-orbital sinuses of the anesthetized rats in sterile tubes using heparinized capillary tubes[15] for measuring serum calcium, phosphorus, bone-specific alkaline phosphatase (BALP), and tartrate-resistant acid phosphatase (TRAP) levels among the overnight fasted rats of the studied groups[16].

The levels of calcium and phosphorous were measured using an automated colorimetric technique (Biodiagnostic Company, Egypt), while BALP and TRAP levels were assessed by the enzyme-linked immunosorbent assay (ELISA) using commercially available kits (CSB-E11865r

and NPB2-76464; CUSIA Bio BIOTECH CO., Houston, USA), respectively[17,18] at the Pharmacognosy Department, Faculty of Pharmacy (Boys), Al Azhar University, Cairo, Egypt. Results for calcium and phosphorus were given in mg/dl, while those for BALP and TRAP were given in IU/L and ng/ml[16,18].

The femurs were dissected out and fixed in buffered formaldehyde 10% for 4 days, then decalcified using formic acid 10%. The decalcified specimens had been processed to obtain paraffin sections of 5μm thickness and were then stained with:

- Hematoxylin and Eosin (H&E) for studying the general structure.
- Masson's trichrome stain for staining the collagen fibers.
- Periodic acid Schiff's (PAS) technique for studying the cement substances of bone trabeculae (glycoproteins and glycosaminoglycans)[19].

Immunohistochemical technique

Immunohistochemical techniques were used to detect the protein expression of receptor activator of nuclear factor-κB ligand (RANKL) and osteopontin (OPN) in formalin-fixed bone tissue sections in the different experimental groups using avidin-biotin immunoperoxidase techniques[20,21]. They were performed at the Cancer Institute, Cairo.

Positively charged 5-μm sections proceeded to deparaffinization in xylene and hydration in descending grades of ethanol, and afterwards endogenous peroxidase was blocked using 0.3% hydrogen peroxide (0.3% H_2O_2) for 30 min., and then a serum blocking solution of 5% normal goat serum (cat. no. ZLI9022; Beijing Zhongshan Golden Bridge) was applied in a moist chamber for 30 min. at room temperature prior to incubation with the primary antibody

The bone sections recognizing RANKL were subsequently incubated overnight at 4˚C with primary antibody using mouse anti-RANKL monoclonal antibody (1:800 dilution; cat. no. ALX-804-244-C100, Alexis Biochemicals, San Diego, CA, USA). While the bone sections recognizing OPN were incubated using rabbit anti-OPN polyclonal antibody (1:200 dilution; cat. no. ab8448; Abcam, Cambridge, MA, USA) in humidified chambers following the manufacturer's instructions[20,21]. The sections were incubated with biotinylated secondary antibodies (goat anti-rabbit/mouse immunoglobulin G) (Dako Ltd., diluted 1:200) for the corresponding primary antibody, and thereafter sections were incubated with the avidin–biotin-conjugated peroxidase complex (Vector Laboratories Ltd., UK) for 15 min. Visualisation of the antigen-antibody reaction by incubating bone sections in 3,3'-diaminobenzidine-substrate chromagen (DAB) solution 0.05% (Sigma Chemical Co., Poole, UK) for 15 min. Subsequent counterstaining with Mayer's hematoxylin for 5 sec, was conducted, dehydrated, and mounted with DPX.

A positive RANKL immune reaction reveals cytoplasmic brown punctuations or granular staining substances. While a bone section with an extracellular localization of brown punctuates or granular staining substances in the bone matrix was considered OPN-positive immune reactive.

Positive control slides were applied (Figures 1a,b). Negative control for RANKL and OPN was achieved by replacing the primary antibody with PBS (Figures 1c,d).

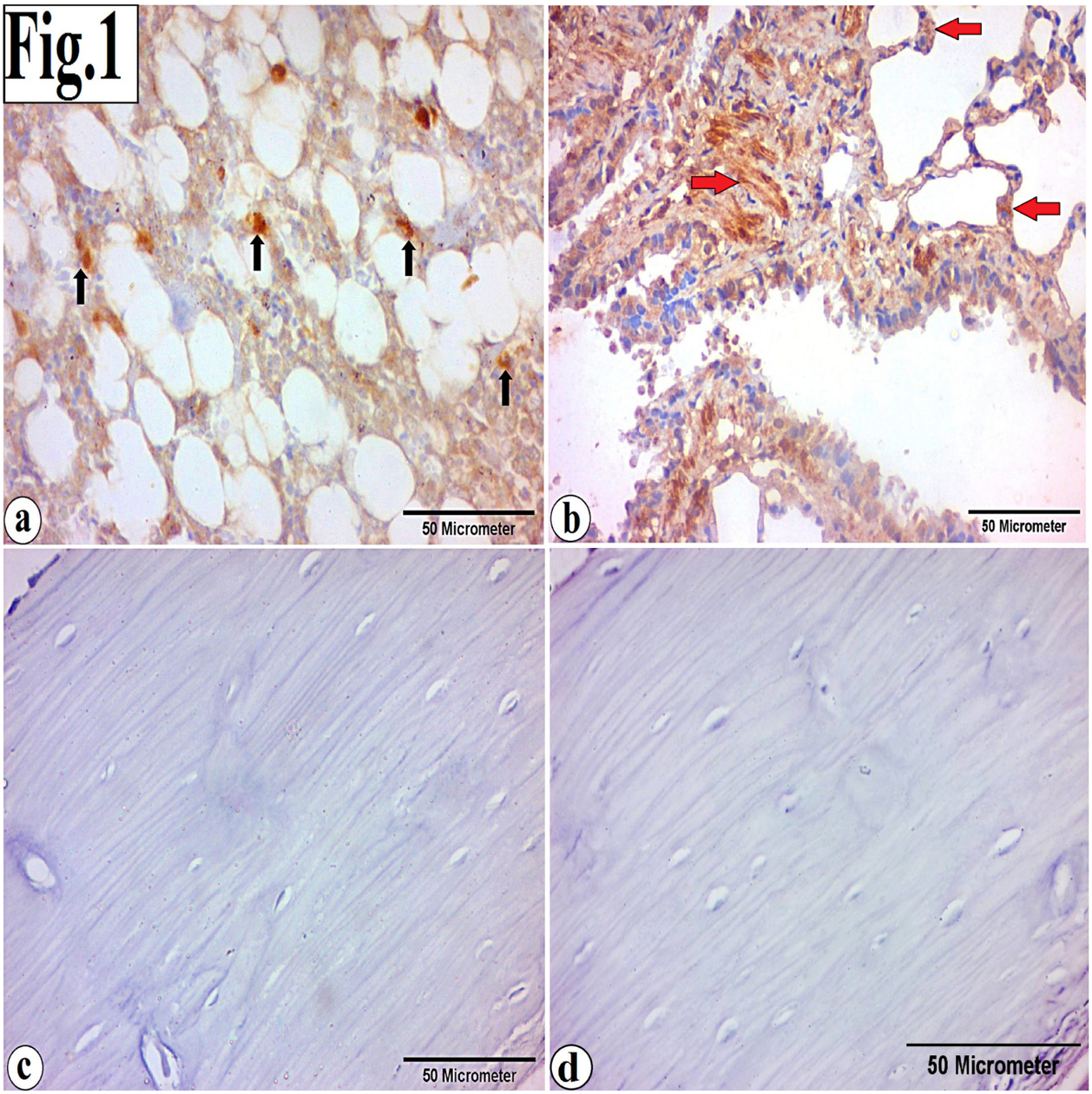

Fig. 1: Photomicrographs of the immunohistochemical reaction: (a) Positive RANKL immune expression in the bone marrow section shows a dark brown reaction within the cytoplasm of the immunogenic cells (black arrows). (b) Positive OPN immune expression in the lung section shows a dark brown reaction within the cytoplasm of the type II pneumocytes and fibroblasts of interstitial tissue (red arrows). (c, d) Negative controls for RANKL and OPN, respectively, in the femurs' shafts where the primary antibodies are omitted. [Immunohistochemical technique; (a, b, c & d) x 400, scale bar = 50 µm]

Quantitative, Morphometric, and Statistical Studies

Various quantitative morphometric parameters were detemined in bone sections, including; the osteocyte count at X200 magnification, the cortical bone thickness in micrometers from the periosteum to the endosteum at five different points spaced 0.5 mm apart in each section, 0.2 mm below the lowest point of the growth plate[22], the area percentage (%) of the thickness of bone trabeculae, and the thickness of the epiphyseal cartilage plate in the hematoxylin and eosin stained sections, all at X100 magnification. Additionally, in the Masson trichrome and PAS-stained sections, respectively, the area % of collagen fibers and the optical density of the PAS-positive cement ground matrix were measured at X200 magnification. Finally, the area % of RANKL and OPN immune expression in the immunohistochemically treated sections at x200 magnification was also detected. Non-overlapping randomly selected 10 fields from five sections of each rat in each group were chosen and morphometrically analyzed using Leica light microscope MDLSD and image analysis software at the Regional Center for Mycology and Biotechnology (RCMB), Al-Azhar University, Cairo, Egypt.

All data were statistically represented in mean ± SD. The one-way analysis of variance (ANOVA) and Tukey's post hoc test were used to compare them. The *P-value* < 0.05 was used as the significant value. The Statistical Package for the Social Sciences, Version 22 for Windows (California, USA), was used to apply the statistical analysis.

RESULTS

Histological results

Hematoxylin and Eosin (H&E) stain (Figures 2-8)

H&E-stained sections from the femurs' shafts of the control and sham-operated groups (GI and GII) displayed nearly similar results in the periosteum, endosteum, and the acidophilic matrix of compact bone in between (Figures. 2a,b). The compact bone showed concentrically arranged bone lamellae, osteocytes in their lacunae between lamellae, as well as centrally located Haversian canals lined by osteoprogenitor cells that made up the Haversian system. External, internal, and interstitial bone lamellae were also seen (Figure 2b). The periosteum consisted of an outer fibrous layer formed of dense collagen fibers with fibroblasts in between, and an inner osteogenic layer made up of spindle-shaped osteoprogenitor cells with elongated nuclei and osteoblasts (Figure 2c). A single layer of osteoprogenitor cells with flat nuclei and osteoblasts with nearly rounded nuclei appeared lining the endosteum (Figure 2d).

Normal trabecular bone architecture consisted of thick interconnected bony trabeculae containing numerous osteocytes entrapped within their lacunae, surrounded bone marrow cavities containing a large number of hemopoietic cells, and were lined by the endosteum, formed mainly of osteoprogenitor cells and osteoblasts (Figures 3a,b).

Well-organized epiphyseal cartilage appeared to be formed of histologically distinct zones, including the resting zone of small and randomly distributed chondrocytes, the proliferative zone of organized adjacent columns of stacked chondrocytes, the hypertrophy zone of enlarged chondrocytes, and the calcification zone, whic contained empty lacunae (Figure 3c).

H&E stained sections from the osteoporotic group (GIIIa) showed different degrees of osteoporosis and loss of normal bone architecture in the form of large bony tunnels (Figure 4a), apparent decreased and irregular cortical bone thickness, thickened outer fibrous layer of the periosteum, osteoporotic cavities, a non-homogenous acidophilic matrix with focal faintly stained regions, and irregular basophilic areas in between, areas devoid of osteocytes, and irregularly arranged osteocytes. The endosteum displayed an irregularly eroded surface (Figures 4b,c,d).

The osteoporotic group (GIIIa) also revealed deteriorated cancellous bone in the form of discontinuous, thin, widely separated bone trabeculae with a non-homogenous acidophilic matrix containing basophilic irregular areas. There were blind-ended trabeculae associated with minor fractures and fissures, as well as islets of very small bone trabeculae representing button phenomena. Wide bone marrow spaces were evident between trabeculae, containing abundant adipocytes and fewer hemopoietic cells than in the control group (Figures 5a,b). Additionally, some empty lacunae in the bone trabeculae were detected (Figure 5c).

The epiphyseal cartilage of the GIIIa exhibited a marked reduction in thickness and appeared disorganized with disruption in the chondrocyte's columnar arrangement. Comparatively to the control group, some homogenous regions of the cartilaginous matrix lacked chondrocytes (Figure 5d).

Inversely, examination of the H&E-stained sections from all treated groups, including the Fosamax-treated group (GIIIb), the Mena Q-treated group (GIIIc), the Fennel-treated group (GIIId), and the combined Mena Q and Fennel-treated group (GIIIe), revealed some improvement in bone structure, with a noticeable increase in cortical bone thickness concurrent with a decrease in the thickness of the outer fibrous layer of the periosteum and the presence of irregular basophilic cement lines indicating new bone formation. Osteocytes of normal shape and distribution were evident between the regularly arranged bone lamellae in the Haversian system (Figure 6a-d). Few osteoporotic cavities, basophilic areas within the acidophilic bone matrix, and slight endosteal erosions were found only in GIIIb, GIIIc, and GIIId (Figures 6a,b,c). Furthermore, the Fennel-treated group (IIId) displayed a thick inner osteogenic layer of the periosteum and a subperiosteal groove in the underlying bone lamellae (Figure 6c). On the other hand, GIIIe showed marked improvement with the preservation of nearly normal bone histoarchitecture (Figure 6d).

The femurs' epiphyses of the treated groups (GIIIb, GIIIc, GIIId, and GIIIe) showed thick and relatively thin interconnected irregular bone trabeculae with wide bone marrow cavities between them containing hematopoietic cells. Bone trabeculae contained osteocytes within their lacunae. They were lined by the endosteum. Few osteoporotic cavities were also observed within the bone trabeculae (Figures 7a-d). Basophilic areas were observed in GIIIc (Figure 7b), while GIIId revealed disconnected bone trabeculae, more osteoporotic cavities, and endosteal erosions (Figure 7c). GIIIe displayed the best histological result and a regular continuous endosteum, however, few osteoporotic cavities were found within the bone trabeculae (Figure 7d).

In the treated groups (GIIIb, GIIIc, and GIIId), the epiphyseal cartilage appeared well-organized with the preservation of chondrocyte arrangement in the different histological zones, except for some regions that appeared devoid of chondrocytes (Figures 8a,b,c). While GIIIe revealed restoration of the cartilage plate's normal thickness as well as nearly normal chondrocytes arranged in the different histological zones comparable to the control group (Figure 8d).

Masson's trichrome stain (Figures 9-11)

Masson's trichrome-stained bone sections from the femur of the control and sham-operated groups (GI & GII) showed the normal distribution of the collagen fibers within the periosteum and closely packed fibers within the bone matrix of the diaphysis (Figure 9a). Normal collagen fiber distribution was also detected in the matrix of the cancellous bone trabeculae within the epiphysis of both groups (Figure 9b).

While in the osteoporotic group (GIIIa), an apparently thickened periosteum with a predominant outer fibrous layer and few irregular distributions of the collagen fibers were evident within the bone matrix, as shown by the faint green coloration of the bone matrix. Abnormal collagen fibers at the endosteal surface could be detected (Figure 9c). Additionally, an apparent decrease in the collagen fibers distribution in the bone trabecular matrix within the epiphysis was also observed (Figure 9d).

Inversely, examination of the Masson's trichrome-stained sections from all treated groups (GIIIb, GIIIc, GIIId, and GIIIe) showed a reduction in the thickness of the periosteum's outer fibrous layer and a densely packed collagen fibers distribution in the compact bone matrix that was quite similar to the control (Figures 10a-d). On the other hand, compared to the control group, there was a slight reduction in the collagen fibers distribution in the matrix of the bone trabeculae of the femur's epiphysis in the GIIIb, GIIIc, and GIIId (Figures 11a,b,c). While the bone trabeculae in the GIIIe had more collagen fibers distributed throughout the matrix that appeared more or less similar to the control group (Figure 11d).

Periodic acid Schiff technique (Figures 12-14)

PAS-stained sections from the femurs of the control and sham-operated groups (GI and GII) showed an intense PAS-positive reaction in the cement lines within the compact bone matrix (Figure 12a) and in the cancellous bone trabeculae (Figure 12b).

The osteoporotic group (GIIIa) showed few ill-defined PAS-positive cement lines within the bone matrix of the shaft (Figure 12c) and in the matrix of thin discontinuous bone trabeculae within the epiphysis comparable to the control group (Figure 12d).

Inversely, examination of the PAS-stained sections from all treated groups (GIIIb, GIIIc, GIIId, and GIIIe) displayed a nearly normal PAS-positive reaction with an intense reaction in the cement lines distributed throughout the compact bone matrix of the shaft (Figures 13a–d) and in the cancellous bone trabeculae of the femur's epiphysis that appeared more or less similar to the control group (Figures 14a –d).

Immunohistochemical results (Figures 15-21)

Immunohistochemical results for receptor activator of nuclear factor-κB ligand (RANKL)

RANKL immune expression was undetectable in the compact bone matrix of the femurs' shafts and the cancellous bone trabeculae of the control (GI) and sham-operated (GII) groups (Figures 15a,b).

While in the osteoporotic group (GIIIa), strong positive RANKL immune expression was detected in the osteoporotic cavities, within the endosteum of the femurs' shafts (Figure 15c), and in the trabecular bones' endosteum of the femurs' epiphyses (Figure 15d).

In contrast, examination of the femur sections of the treated groups (GIIIb, GIIIc, and GIIId) revealed a mildly positive RANKL immune expression in the osteoporotic cavities within the compact bone matrix of the shaft (Figures 16a,b,c). While GIIIe displayed a faint RANKL immune expression in the compact bone matrix (Figure 16d). As regards the femurs' epiphyses, all treated groups IIIb, IIIc, IIId, and IIIe displayed weak RANKL immune expression in the endosteum of the trabecular bone (Figures 17a –d).

Immunohistochemical results for osteopontin (OPN)

Positive osteopontin (OPN) protein immune expression was detectable as brown granules in the bone matrix with increased inductive effect around osteoblasts at the periosteum, in the cement lines of the shaft, around the osteocytes resident in lacunae, around the Haversion canals, as well as at the endosteal surface close to the bone marrow (Figures 18a–c). Strongly positive osteopontin was also detected in the cement lines of the femur's trabeculae in the control (GI) and sham-operated (GII) groups (Figure19a).

OPN immunohistochemical staining of the femur sections of the osteoporotic rats (GIIIa) revealed a decreased osteoinductive effect around the osteoblasts and osteocytes as evidenced by a weak osteopontin protein immune reactivity within the bone matrix of the femur's shaft (Figure 18d). On the other hand, other sections showed strong positive osteopontin immune expression within the degenerative areas, osteoporotic cavities, and at the endosteum of the femur's shaft (Figures 18e–g). Additionally, weak OPN immune expression was also detected in the cement lines of the bone trabeculae of the osteoporotic group (Figure 19b).

Inversely, examination of the femur sections from the treated groups (GIIIb, GIIIc, GIIId, and GIIIe) revealed a nearly normal positive OPN immune expression in the bone matrix and in the cement lines of the femur's shaft and at the endosteal surfaces (Figures 20a–h). Furthermore, strong positive OPN expression was evident in the osteoporotic cavities of GIIIb (Figures 20a,b), GIIIc (Figures 20c,d), and GIIId (Figures 20e,f). Additionally, all treated groups showed strong positive OPN reactions within the bone matrix and in the cement lines of the trabecular bone (Figures 21a–d).

Statistical results

Body weight

All of the studied groups' mean initial body weights (IBW) were quite similar, with no statistically significant values. They varied between 145.8±4.9 and 152.5±5.2

At the end of the experiment, the studied groups' mean final body weights (FBW) significantly increased. The osteoporotic group (GIIIa) had the highest recorded mean of the FBW when compared to the other experimental groups, followed by those of the Fosamax-treated group (GIIIb), Mena Q-treated group (GIIIc), and Fennel-treated group (GIIId). While the control group (I) recorded the least mean of the FBW, followed by the sham-operated group (GII) and then the combined Mena Q and Fennel-treated group (GIIIe), with a statistically significant difference (P<0.05) (Table 1, Histogram 1).

Biochemical results

The statistical study concerning serum calcium, phosphorus, bone-specific alkaline phosphatase (BALP), and tartrate-resistant acid phosphatase (TRAP) among rats of all experimental groups showed that the osteoporotic group (GIIIa) had the least mean values of serum calcium and phosphorus coupled with the highest mean of BALP, and TRAP levels when compared to the other experimental groups (Table 2).

Inversely, the treated groups (GIIIb, GIIIc, GIIId, and GIIIe) enhanced these parameters, as evident by a significant increase in serum calcium and phosphorus along with a significant decrease in both BALP and TRAP levels comparable to the osteoporotic group (GIIIa). Interestingly, the improvement could not reach the control values as there was a significant difference when compared to the control group (P<0.05), with the exception of GIIIe, which recorded significant values when compared with the treated groups IIIc, and IIId (P<0.05) but non-significant values when compared with the control group and GIIIb (p>0.05) (Table 2).

Histomorphometric results

1. The osteocyte count: There was a significant decrease in the mean value of osteocyte count in the osteoporotic group (IIIa), which showed the least value compared to the other experimental groups.

On the other hand, all treated groups (GIIIb, GIIIc, GIIId, and GIIIe) showed a clear improvement with a significant increase in the osteocyte count when compared to the osteoporotic group (P<0.05) with the highest mean value among GIIIe when compared with the other treated groups IIIb, IIIc, and IIId (P<0.05). However, GIIIb, GIIIc, GIIId, and GIIIe showed significantly decreased values when compared with the control group (p<0.05) (Table 3, Histogram 2).

2. The cortical thickness (µm) and the area percentage (%) of the trabecular bone thickness: Comparing the osteoporotic group (IIIa) to the other experimental groups, the osteoporotic group showed the lowest mean values of the cortical thickness and the area % of trabecular bone thickness.

Contrarily, all treated groups (GIIIb, GIIIc, GIIId, and GIIIe) showed a noticeable improvement, with a significant increase in cortical and trabecular bone thickness comparable to the osteoporotic group (P<0.05), however, it could not approach the control values. Interestingly, GIIIe recorded the best improvement, with a significant difference compared to the treated groups IIIb, IIIc, and IIId (P<0.05) but a non-significant value when compared with the control group (p>0.05) (Table 3, Histograms 3,4).

3. The thickness of epiphyseal growth plate cartilage (µm): There was a significant decrease in the mean value of the epiphyseal cartilage plate thickness in the osteoporotic group (IIIa), which recorded the least value compared to the other experimental groups.

On the other hand, as compared to the osteoporotic group, all treated groups (GIIIb, GIIIc, GIIId, and GIIIe) showed a clear improvement with a significant increase in the mean thickness (P<0.05). GIIIe had the highest mean value and showed a non-significant difference when compared with the GIIIb, and the control group (p>0.05), whereas GIIIb, GIIIc, and GIIId showed significantly lower values when compared with the control group (p<0.05) (Table 3, Histogram 5).

The area percentage of collagen fibers in the cortical and trabecular bone matrix: Using Masson's trichrome stained sections, the osteoporotic group (GIIIa) had the lowest mean values for the mean area% of collagen fibers in the cortical and trabecular bone matrix in comparison to the other experimental groups.

All treated groups (GIIIb, GIIIc, GIIId, and GIIIe) showed a marked improvement when compared to the osteoporotic group, with a significant increase in the area% of collagen fibers (P<0.05), but they could not reach the control values and displayed significantly lower values when compared to the control group (p<0.05). Additionally, GIIIe had significantly increased values when compared to GIIIc, and GIIId (P<0.05) but showed non-significantly elevated values when compared to GIIIb (p>0.05) (Table 4, Histogram 6).

The optical density of PAS-positive cement ground matrix in the cortical and trabecular bones: The osteoporotic group (IIIa) showed the lowest mean values of the optical density of the PAS-positive cement ground matrix in the cortical and trabecular bones compared to the other experimental groups in PAS-stained sections.

While all treated groups (GIIIb, GIIIc, GIIId, and GIIIe) showed a clear improvement when compared to the osteoporotic group, there was a significant increase in the mean values (P<0.05) as well as significant values when compared to the control group (P<0.05) with the exception of GIIId, which showed non-significant values when compared to the control group (p>0.05). Additionally,

GIIIe had significantly increased values when compared to GIIIc, and GIIId (P<0.05) but showed non-significantly elevated values when compared to GIIIb (p>0.05) (Table 4, Histogram 7).

The area% of RANKL and osteopontin (OPN) immune expression in the cortical and trabecular bones: Comparing the osteoporotic group (GIIIa) to the other experimental groups, the osteoporotic group had the highest mean area% of RANKL immune expression coupled with the lowest mean area percentage of OPN immune expression in the cortical and trabecular bones.

On the other hand, all treated groups (GIIIb, GIIIc, GIIId, and GIIIe) showed marked improvement, with a significant decrease in RANKL immune expression and a significant increase in OPN expression in the cortical and trabecular bones when compared to the osteoporotic group (P<0.05) as well as significant values when compared to the control group (P<0.05) with the exception of GIIIe, which showed significantly lower RANKL values when compared with the treated groups IIIb, IIIc, and IIId (P<0.05) and significantly higher OPN values only with the GIIId (P<0.05) but showed non-significant values when compared with the control group (P>0.05) (Table 5, Histograms 8, 9).

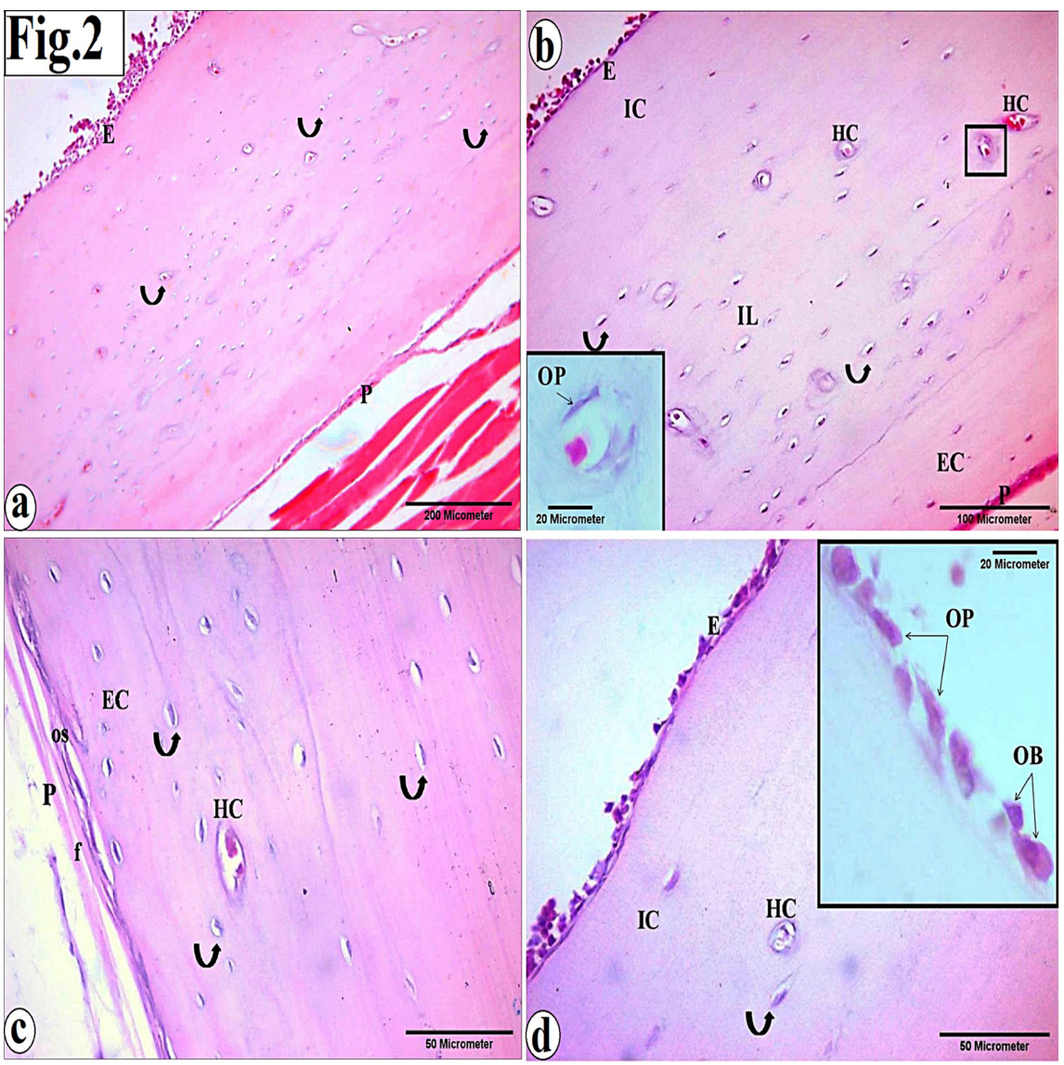

Fig. 2: Photomicrographs of sections from the femurs' shafts of the control group (GI), showing: (a, b) The periosteum (P), endosteum (E), and the acidophilic matrix of the compact bone contain osteocytes (curved arrows). (b) Osteocytes inside their lacunae (curved arrows) are concentrically arranged around centrally located Haversian canals (HC). Internal (IC), external (EC) circumferential lamellae, and interstitial bone lamellae (IL) are also noticed. The inset, a higher magnification of the Haversian canal, shows osteoprogenitor cells (OP) with flat nuclei. (c) The outer fibrous layer (f) and the inner osteogenic layer (os) of the periosteum (P), osteocytes inside lacunae (curved arrows), Haversian canal (HC), and external circumferential lamellae (EC) are seen. (d) Endosteum (E), osteocytes (curved arrows), Haversian canal (HC), and internal circumferential lamellae (IC) are seen. The inset, a higher magnification of the endosteal surface, shows multiple osteoprogenitor cells (OP) with flat nuclei and osteoblasts (OB) with rounded nuclei. [H&E; (a) x100, scale bar = 200 µm, (b) x200, scale bar = 100 µm, (c, d) x400, scale bar = 50 µm, and (inset in b, d) x1000, scale bar = 20 µm].

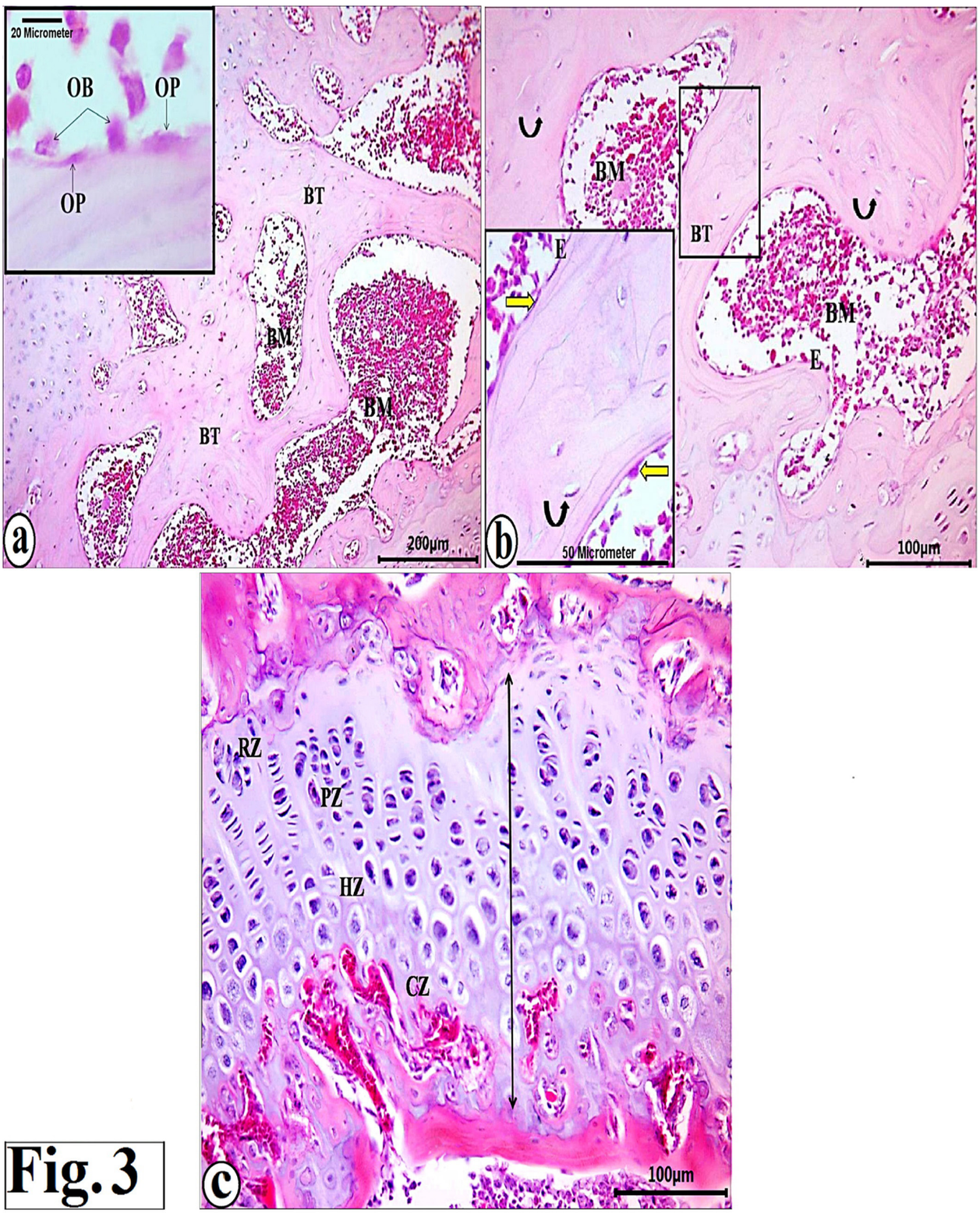

Fig. 3: Photomicrographs of sections from the epiphysis of the femur of a sham-operated rat (GII), showing: (a, b) thick interconnecting cancellous bone trabeculae (BT) with bone marrow spaces (BM) in between contain hemopoietic cells. (a) The inset, a higher magnification of the endosteal surface, shows osteoprogenitor cells (OP) with flat nuclei and osteoblasts (OB) with rounded nuclei. (b) The bone trabecula (BT) contains osteocytes (curved arrows) and is lined by the endosteum (E). The inset at a higher magnification shows osteocytes inside their lacunae (curved arrows), as well as a single layer of osteogenic cells (yellow arrows) lines the endosteum (E). (c) Highly organized epiphyseal cartilage (↕) contains the resting zone of small chondrocytes (RZ), the proliferative zone (PZ) of adjacent chondrocyte columns, the hypertrophy zone (HZ) of enlarged chondrocytes, and the calcification zone (CZ) with empty lacunae. [H&E; (a) x100, scale bar = 200 µm; inset x1000, scale bar = 20 µm, (b) x200, scale bar = 100 µm; inset x400, scale bar = 50 µm , and (c) x200, scale bar = 100 µm].

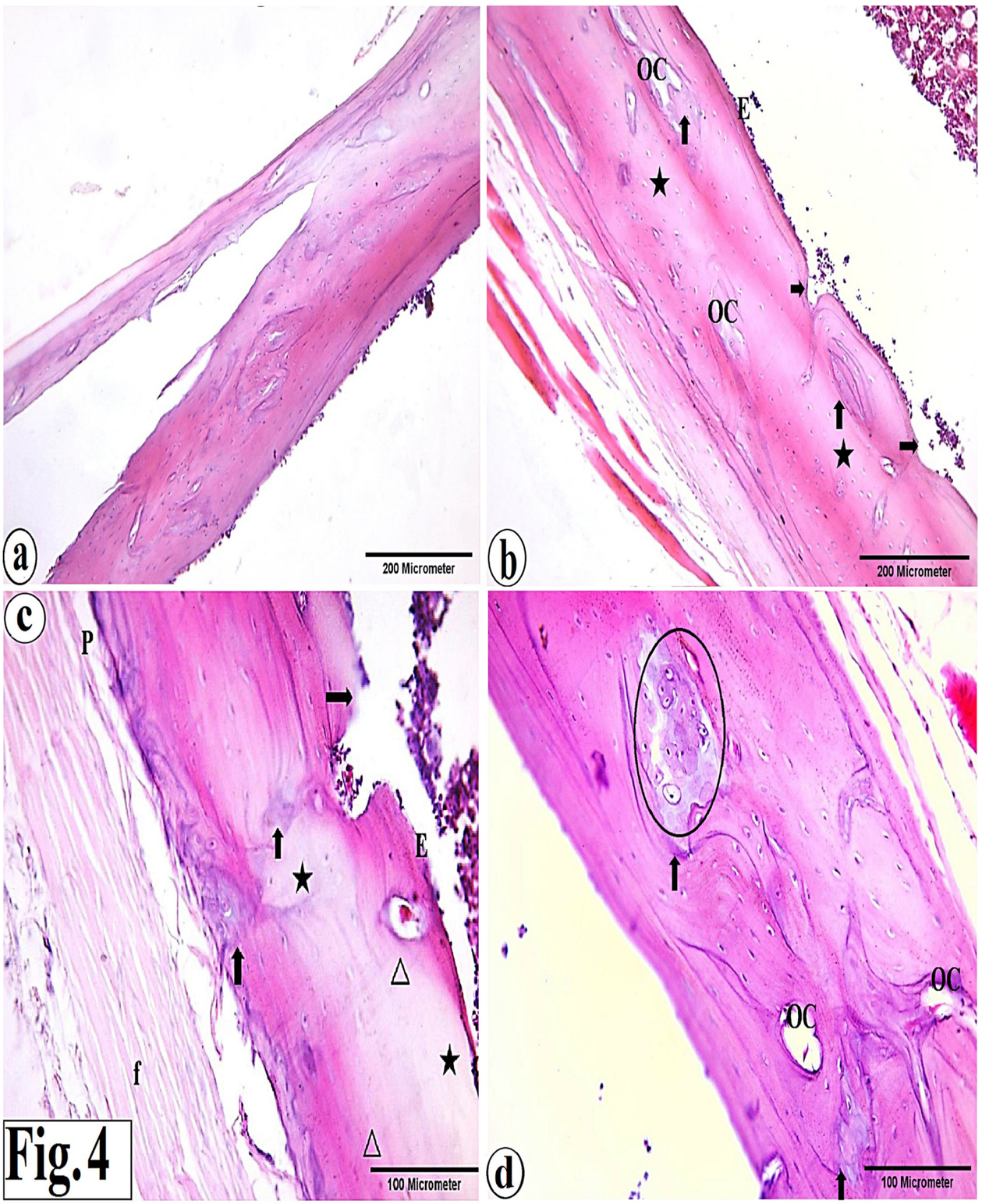

Fig. 4: Photomicrographs of femurs' shaft of the osteoporotic group (GIIIa), showing: (a) large bony tunnel within a compact bone matrix. (b, c) Irregular cortical bone thickness, non-homogenous acidophilic matrix with faintly stained regions (stars), irregular basophilic areas (↑), and erosions (→) of the endosteum (E). (b) Osteoporotic cavities (OC) appear inside the bone matrix. (c) Thick outer fibrous layer (f) of the periosteum (P) and areas devoid of osteocytes (Δ) are noticed in the acidophilic matrix of compact bone. (d) Irregularly arranged osteocytes (circle), basophilic areas (↑), and osteoporotic cavities (OC) are noticed within the compact bone matrix. [H&E; (a, b) x100, scale bar = 200 µm, (c & d) x200, scale bar = 100 µm].

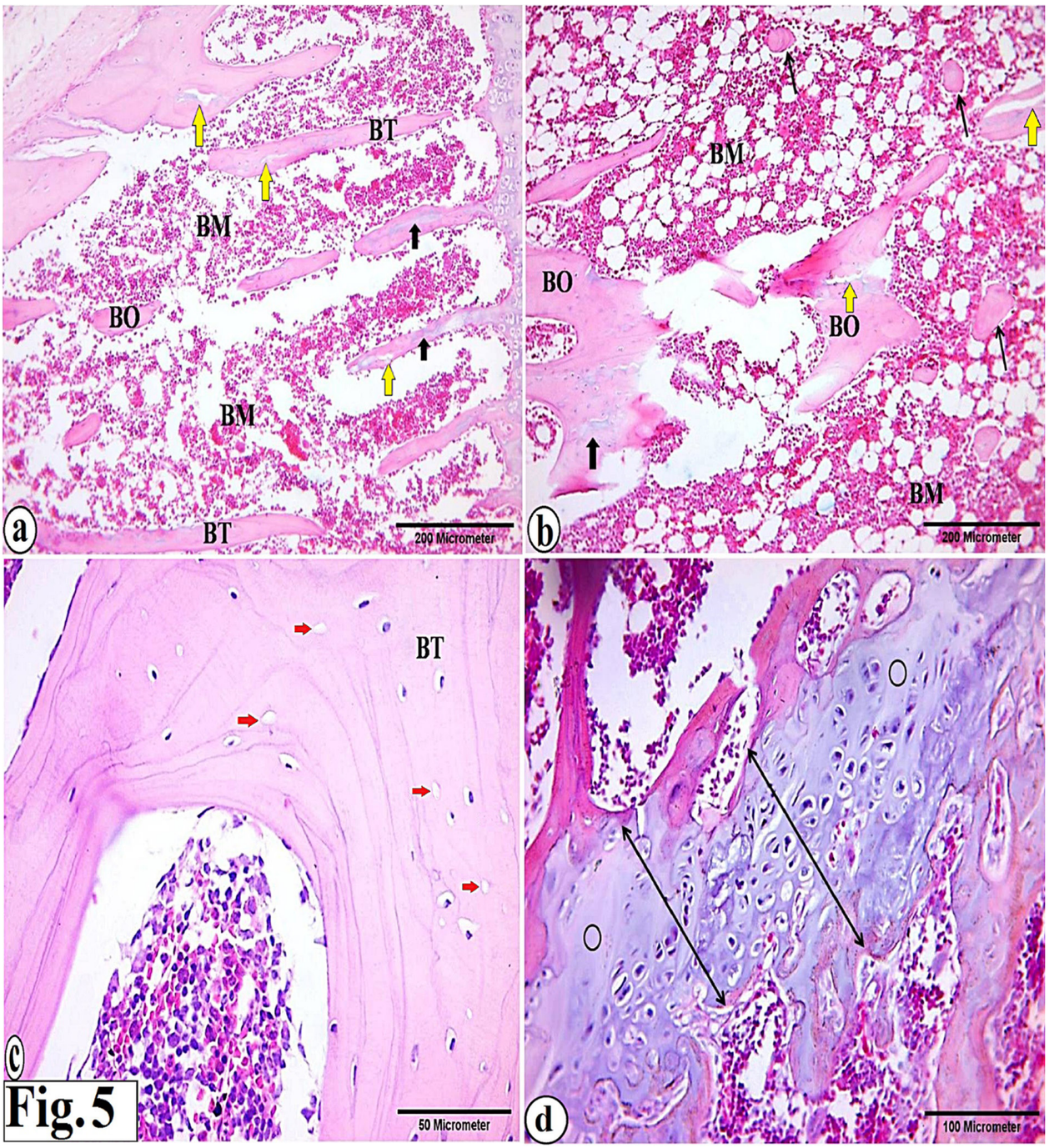

Fig. 5: Photomicrographs of the epiphysis of the femur of the osteoporotic group (GIIIa), showing: (a, b) thin and widely separated bone trabeculae (BT) with minor fissures (yellow arrows) and basophilic areas within the acidophilic bone matrix (thick arrows). Discontinuous bony ossicles (BO) are also seen. (b) Islets of very small trabeculae represent button phenomena (thin arrows), and apparent wide bone marrow spaces (BM) filled with adipocytes are noticed. (c) Some empty lacunae (red arrows) in the bone trabeculae (BT) are seen. (d) A reduction in the cartilage plate thickness (↕), disruption in the chondrocyte's columnar arrangement, and loss of chondrocytes in some areas of the cartilaginous matrix (○) are noticed. [H&E; (a, b) x100, scale bar = 200 µm, (c) x400, scale bar = 50 µm , and (d) x200, scale bar = 100 µm]

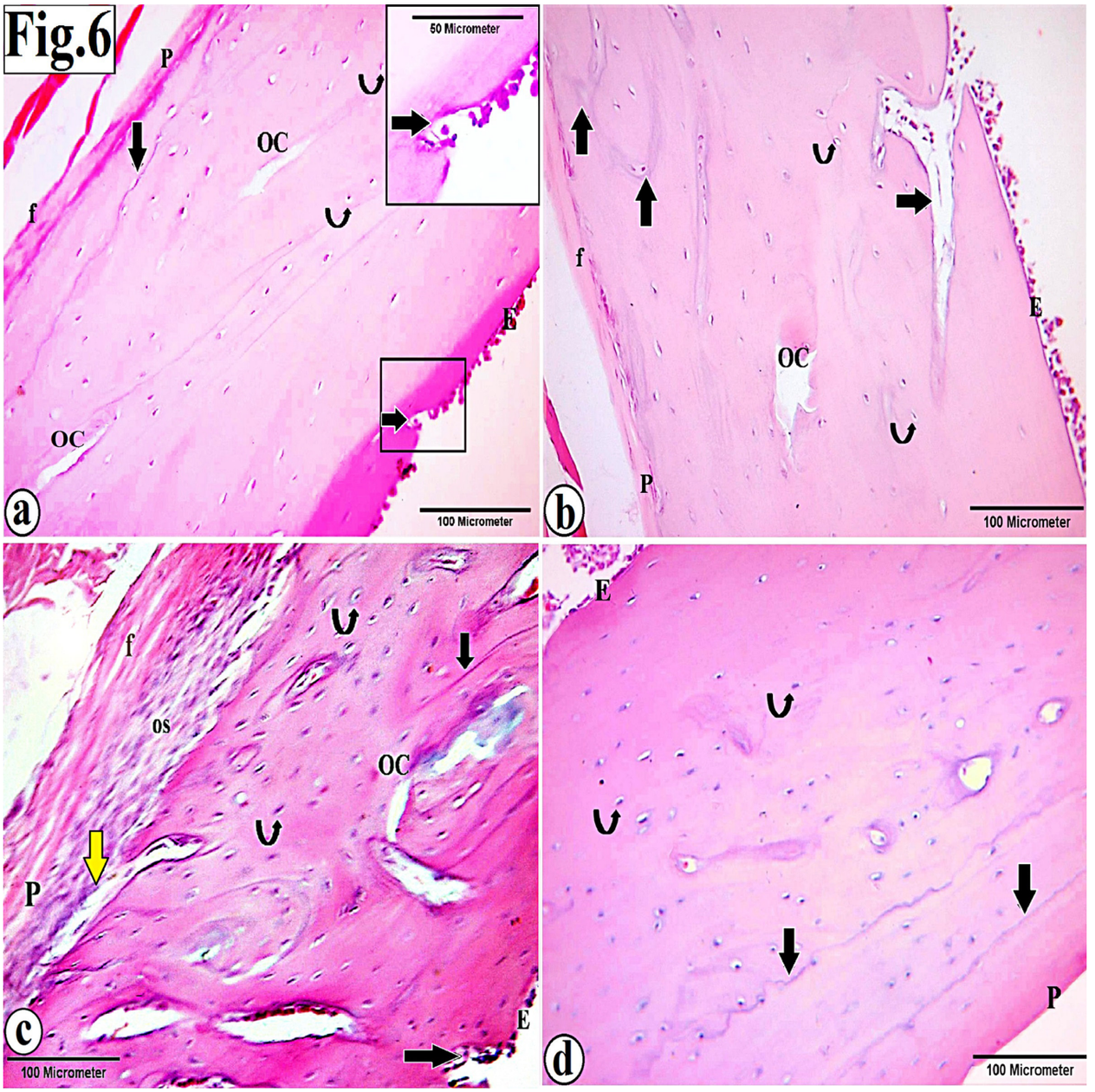

Fig. 6: Photomicrographs of the femurs' shafts of the treated groups; (a) Fosamax-treated group (GIIIb), (b) Mena Q-treated group (GIIIc), and (c) Fennel-treated group (GIIId), showing the outer fibrous layer (f) of the periosteum (P), as well as the normal shape and distribution of osteocytes (curved arrows), with the presence of few osteoporotic cavities (OC) within the compact bone matrix and erosion (→) in the endosteal surface (E). (a) The Fosamax-treated group (GIIIb) exhibits basophilic cement lines (↓) within the acidophilic bone matrix. The inset at a higher magnification shows slight erosion in the endosteum (→). (b) The Mena Q-treated group (GIIIc) shows some basophilic areas (↑) within the acidophilic bone matrix. (c) The fennel-treated group (GIIId) shows a thick inner osteogenic layer (os) of the periosteum (P), a subperiosteal groove (yellow arrows), and basophilic cement lines (↓) within the acidophilic bone matrix. (d)The Mena Q and Fennel-treated group (GIIIe) shows nearly normal periosteum (P), endosteum (E), and normal shape and distribution of osteocytes (curved arrows) in addition to the presence of basophilic cement lines (↓) within the acidophilic matrix of the compact bone. [H&E; (a, b, c & d) x200, scale bar = 100 µm, and (inset in a) x400, scale bar = 50 µm].

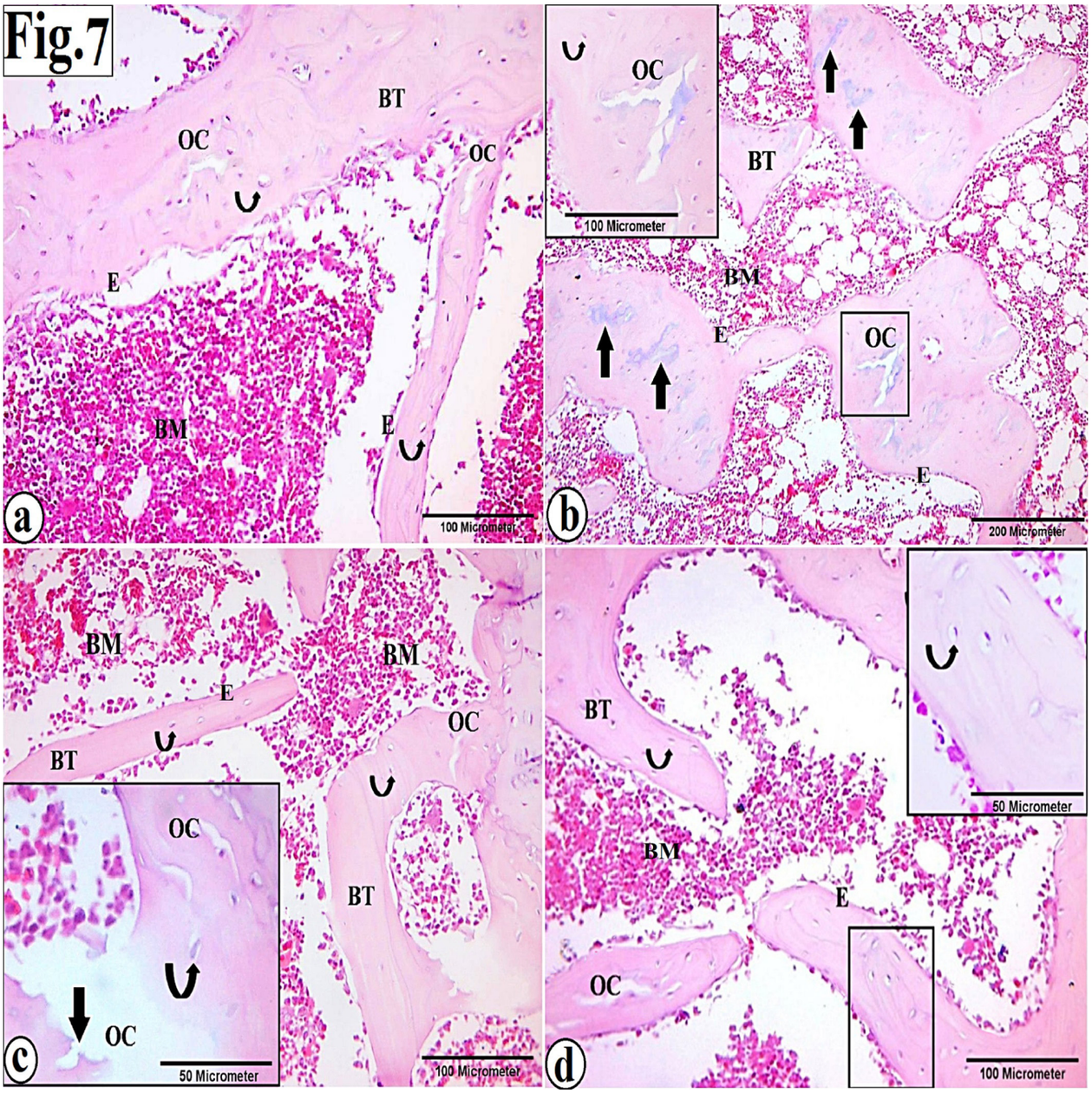

Fig. 7: Photomicrographs from the epiphysis of femurs of the treated groups; (a) Fosamax-treated group (GIIIb), (b) Mena Q-treated group (GIIIc), (c) Fennel-treated group (GIIId), and (d) Mena Q and Fennel-treated group (GIIIe), showing: cancellous bone's trabeculae (BT) contain randomly distributed osteocytes (curved arrows) and enclosed bone marrow cavities (BM) that are lined by the endosteum (E). Few osteoporotic cavities (OC) within the acidophilic bone matrix are also seen. (b) The Mena Q-treated group (GIIIc), shows some basophilic areas (↑) inside thick bone trabeculae (BT). The inset, at a higher magnification, shows normal osteocytes (curved arrows) in lacunae and osteoporotic cavity (OC) within the bone trabeculae. (c)The fennel-treated group (GIIId) shows disconnected bone trabeculae (BT). The inset, at a higher magnification, shows the osteocytes (curved arrows), osteoporotic cavities (OC), endosteal erosion (↓) and the disconnected bone trabeculae. (d) The Mena Q and Fennel-treated group (GIIIe) show regular continuous endosteum (E). The inset, at a higher magnification, shows normal osteocytes (curved arrows) trapped in lacunae within the trabecular matrix. [H&E; (a, c & d) x200, scale bar=100 µm, (b) x100, scale bar = 200 µm; (inset in b) x200, scale bar = 100 µm , and (inset in c, d) x 400, scale bar = 50 µm].

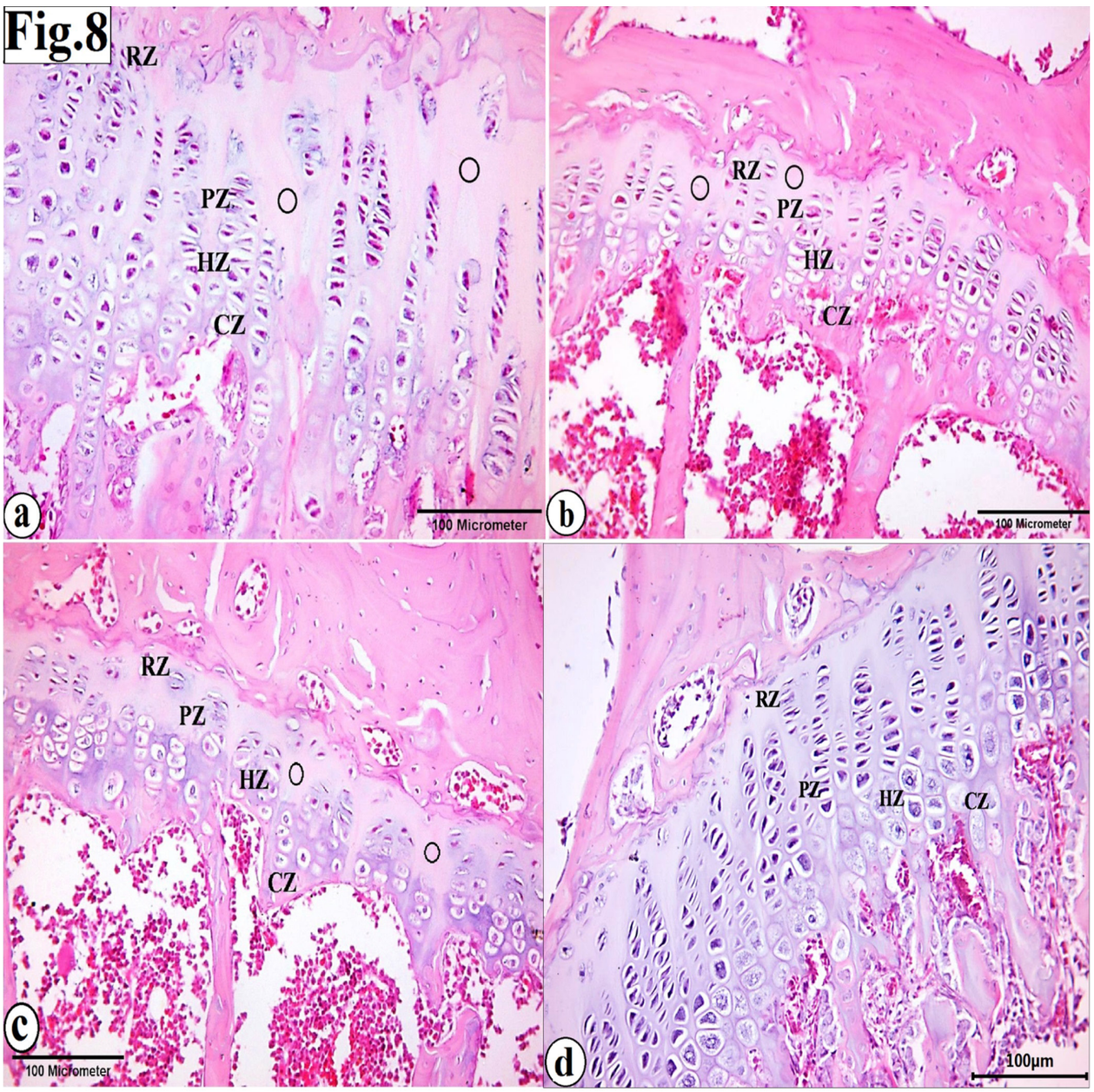

Fig. 8: Photomicrographs of sections from the epiphyseal growth plates of the treated groups: (a) Fosamax-treated group (GIIIb), (b) Mena Q-treated group (GIIIc) (c) Fennel-treated group (GIIId), showing: well-organized epiphyseal cartilage, chondrocyte arrangement in the resting zone (RZ), stacked chondrocyte columns in the proliferative zone (PZ), enlarged chondrocytes in the hypertrophy zone (HZ), and empty lacunae in the calcification zone (CZ). Some areas appear devoid of chondrocytes (○). (d) Mena Q and Fennel-treated group (GIIIe), demostrating well-organized epiphyseal cartilage and chondrocyte arrangement in the RZ, PZ, HZ, and CZm which appear more or less as the control group. [H&E; (a, b, c & d) x200, scale bar = 100 µm].

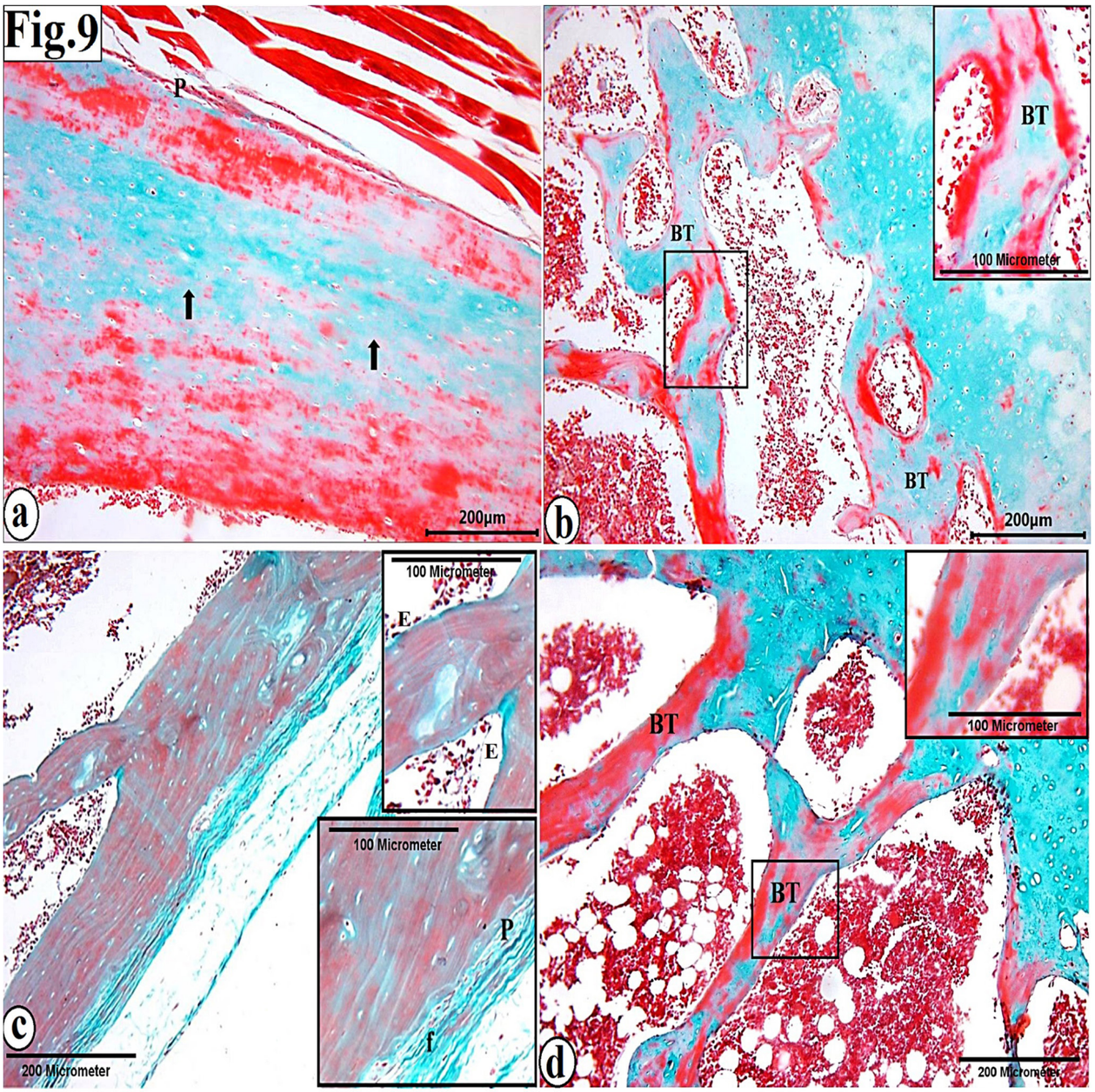

Fig. 9: Photomicrographs of sections from the femurs' shaft and epiphysis of the control and the osteoporotic groups: (a, b) Control group (GI), showing: apparent normal periosteal thickness (P), closely packed bundles (green color) of the collagen fibers (↑) within the reddish bone matrix of the shaft, and within the bone trabeculae (BT). The inset, at a higher magnification, shows a normal distribution of the collagen fibers within the bone trabeculae (BT). (c, d) The osteoporotic group (GIIIa), showing: a decrease in the collagen fibers distribution within the matrix of the shaft of compact bone and within the thin bone trabeculae (BT). Insets, at higher magnifications, show an increase in the thickness of the outer fibrous layer (f) of the periosteum (P), an abnormal presence of collagen fibers along the endosteal surface (E), and a decrease in the distribution of collagen fibers within the bone trabecular matrix. [Masson's trichrome; (a, b, c, d) x100, scale bar = 200 µm, and (inset in b, c, d) x200, scale bar = 100 µm].

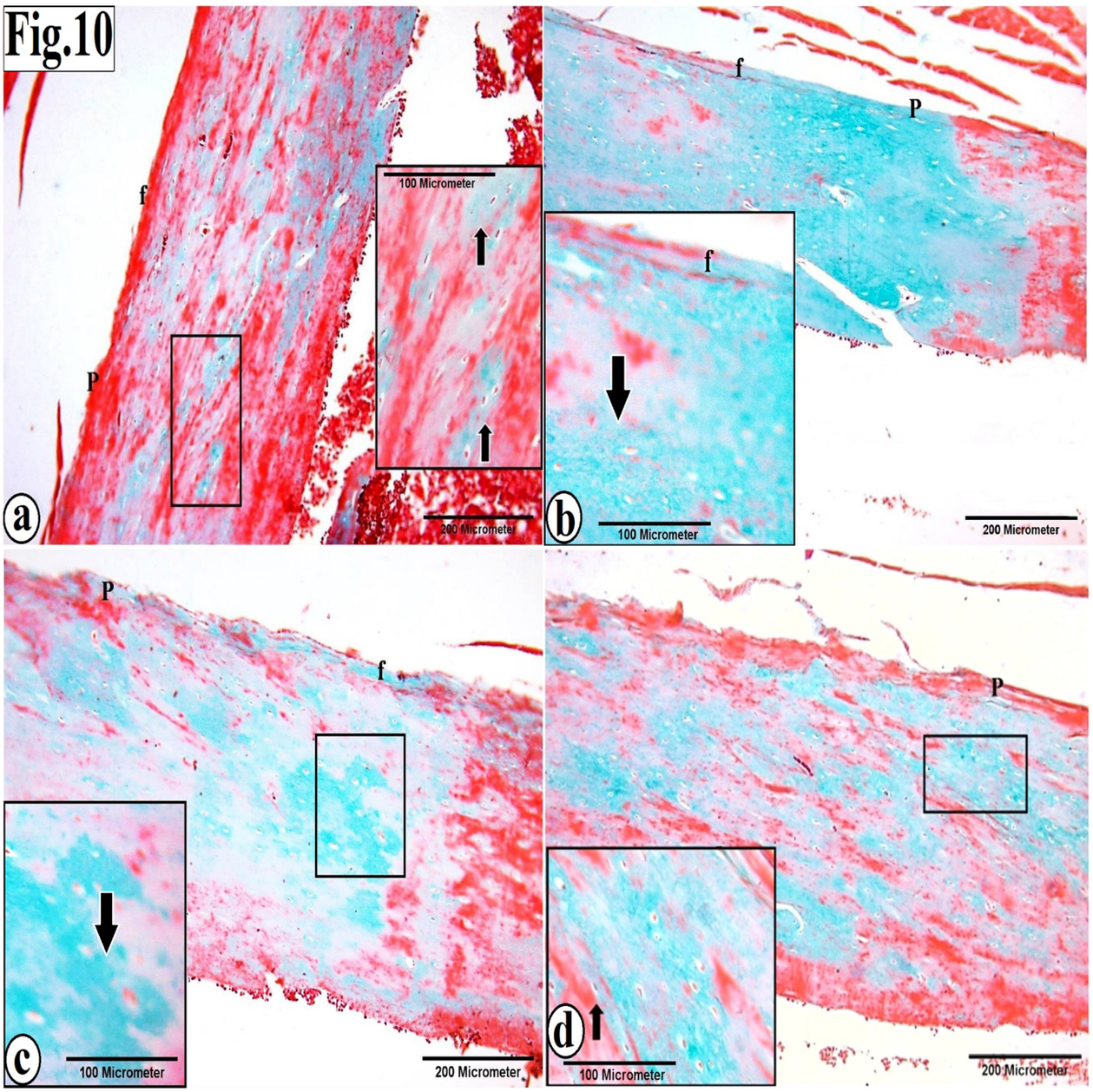

Fig. 10: Photomicrographs of sections from the femurs' shafts of the treated groups; (a) Fosamax-treated group (GIIIb), (b) Mena Q-treated group (GIIIc), (c) Fennel-treated group (GIIId), and (d) Mena Q and Fennel-treated group (GIIIe) showing: reduced thickness of the outer fibrous layer (f) of the periosteum (P) and increased collagen fibers distribution (green color) within the reddish bone matrix nearly as the control group. The insets, at higher magnifications, show the dense collagen fibers distribution (arrows) within the compact bone matrix. [Masson's trichrome; (a, b, c & d) x100, scale bar=200 µm & (insets) x200, scale bar=100 µm].

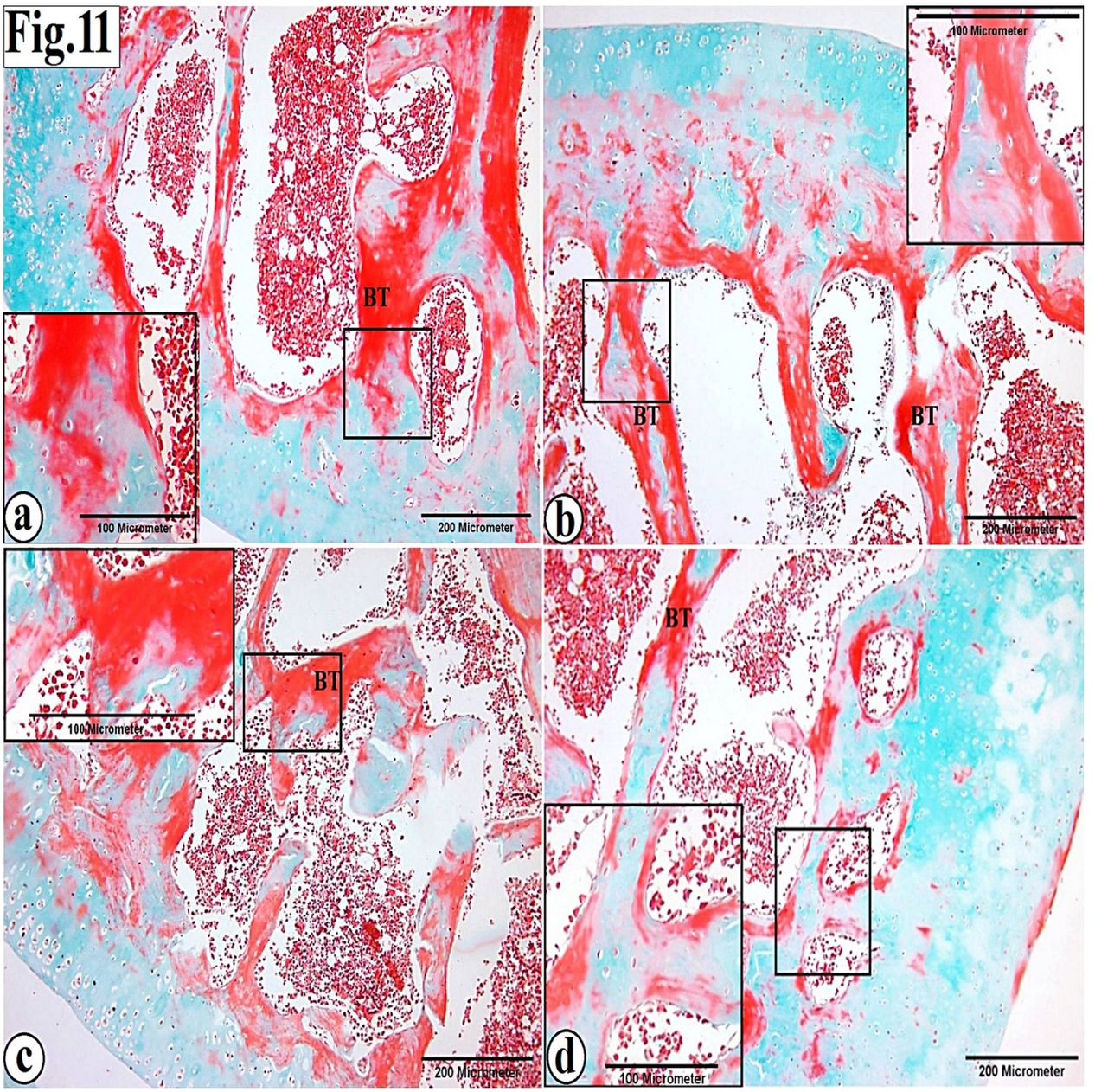

Fig. 11: Photomicrographs from the femurs' epiphyses of the treated groups (a) GIIIb, (b) GIIIc, and (c) GIIId, showing: a slight reduction in the collagen fibers distribution (green color) in bone trabeculae (BT) in comparison to the control group. (d) GIIIe, demonstrating increased collagen fibers distribution within the bone trabeculae (BT) more or less as in the control group. The insets, at higher magnifications, show collagen fibers distribution within the reddish trabecular bone matrix. [Masson's trichrome; (a, b, c & d) x100, scale bar = 200 µm, and (insets) x200, scale bar = 100 µm].

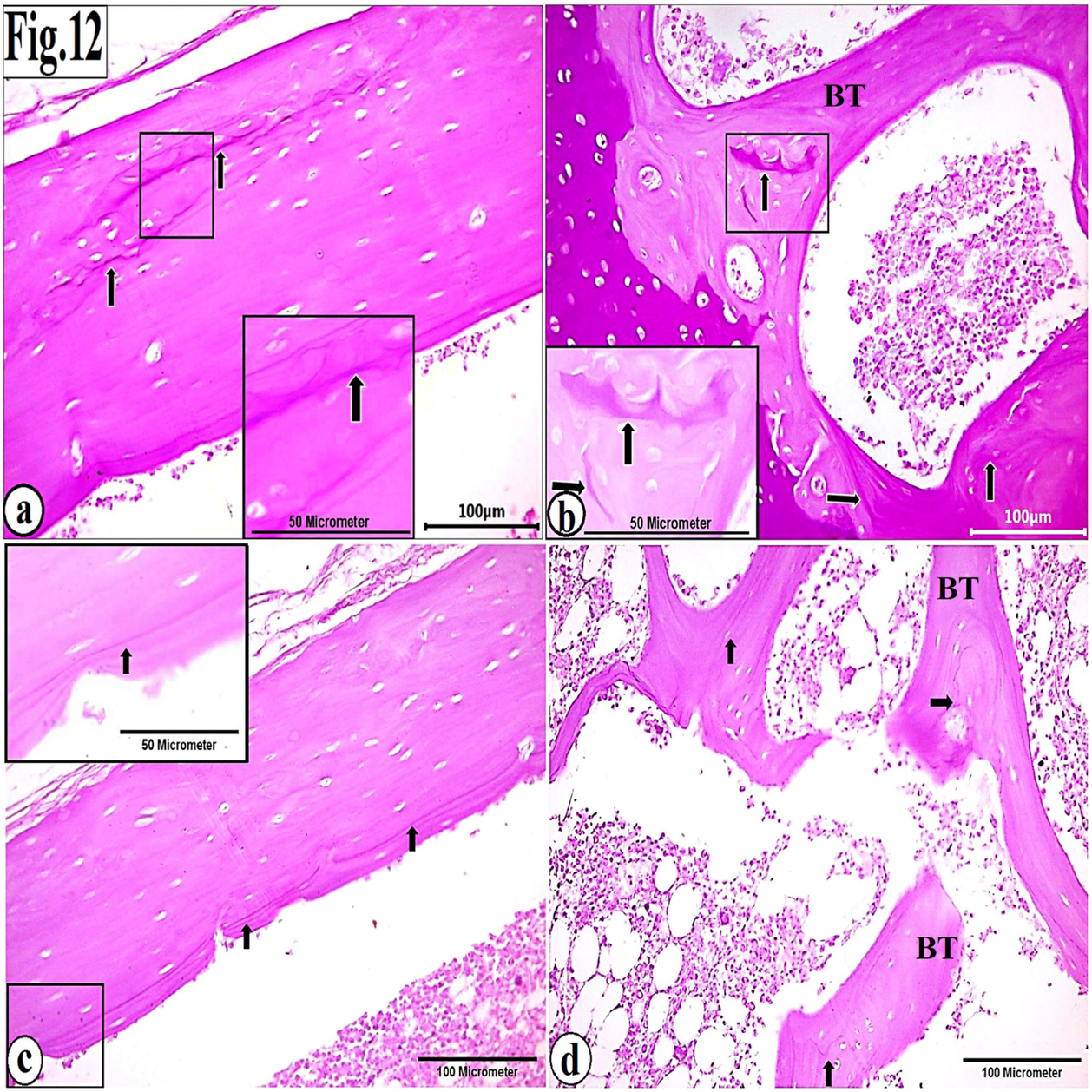

Fig. 12: Photomicrographs of sections from the femurs' shafts and epiphyses of the control and the osteoporotic groups:(a, b) Control group (GI), showing: a PAS-positive reaction (arrows) in the cement lines within the matrix of the compact bone and within the bone trabeculae (BT). (c, d) The osteoporotic group (GIIIa), showing: few ill defined cement lines (arrows) within the matrix of compact bone and within the thin discontinuous bone trabeculae (BT) as compared to the control group. The insets, at higher magnifications of the same regions, show the PAS-positive cement lines within the compact bone and the trabecular matrix. [PAS reaction; (a, b, c, d) x200, scale bar = 100µm , and (inset in a, b & c) x400, scale bar = 50 µm].

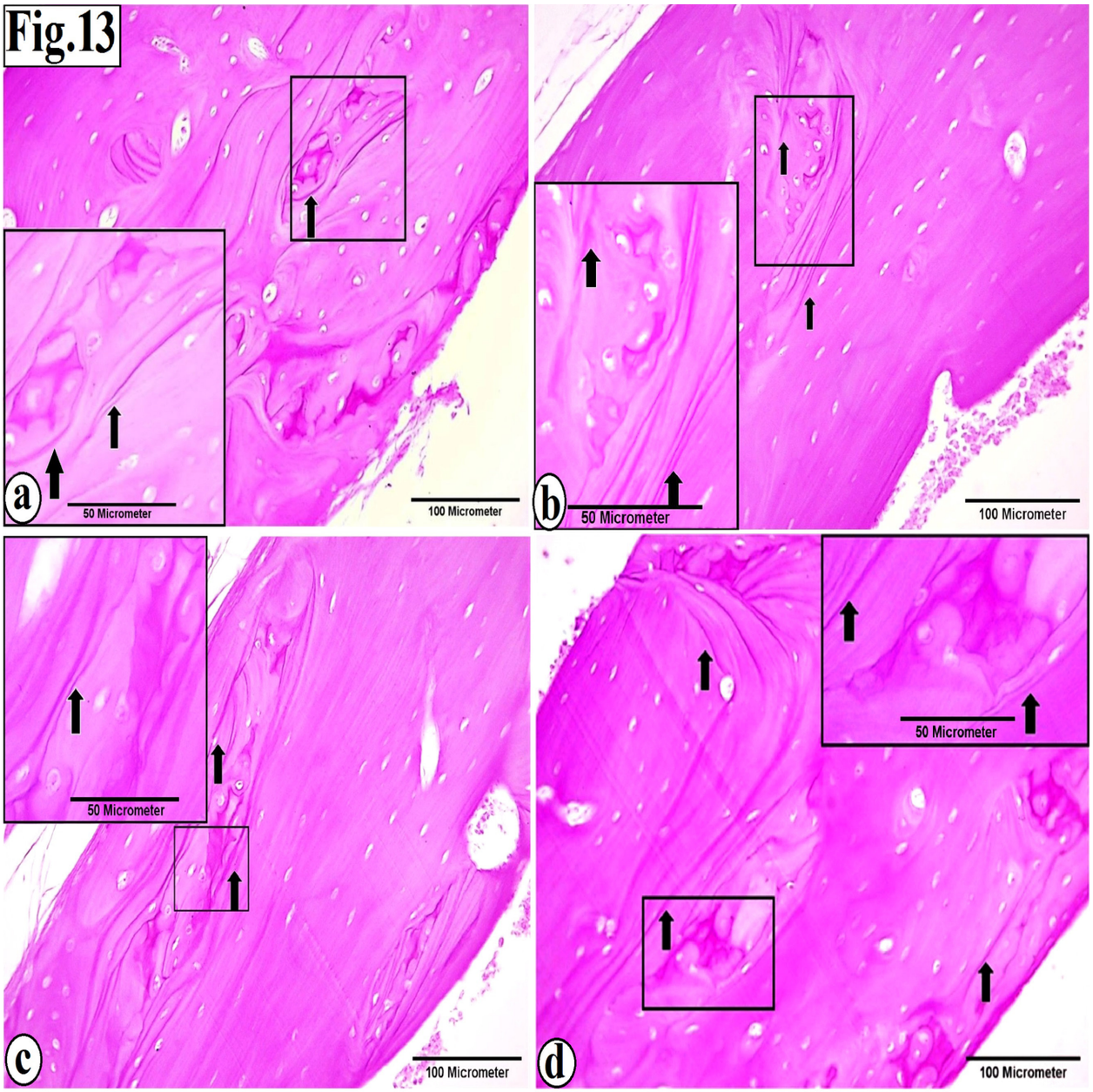

Fig. 13: Photomicrographs from the femurs' epiphyses of the treated groups: (a) Fosamax-treated group (GIIIb), (b) Mena Q-treated group (GIIIc), (c) Fennel-treated group (GIIId), and (d) Mena Q and Fennel-treated group (GIIIe), showing: intense PAS-positive reactions in the cement lines of the compact bone (arrows) of the shaft more or less as the control group. The insets, at higher magnifications, show the PAS-positive cement lines within the compact bone matrix. [PAS reaction; (a, b, c & d) x200, scale bar = 100 µm, and (insets) x400, scale bar = 50 µm].

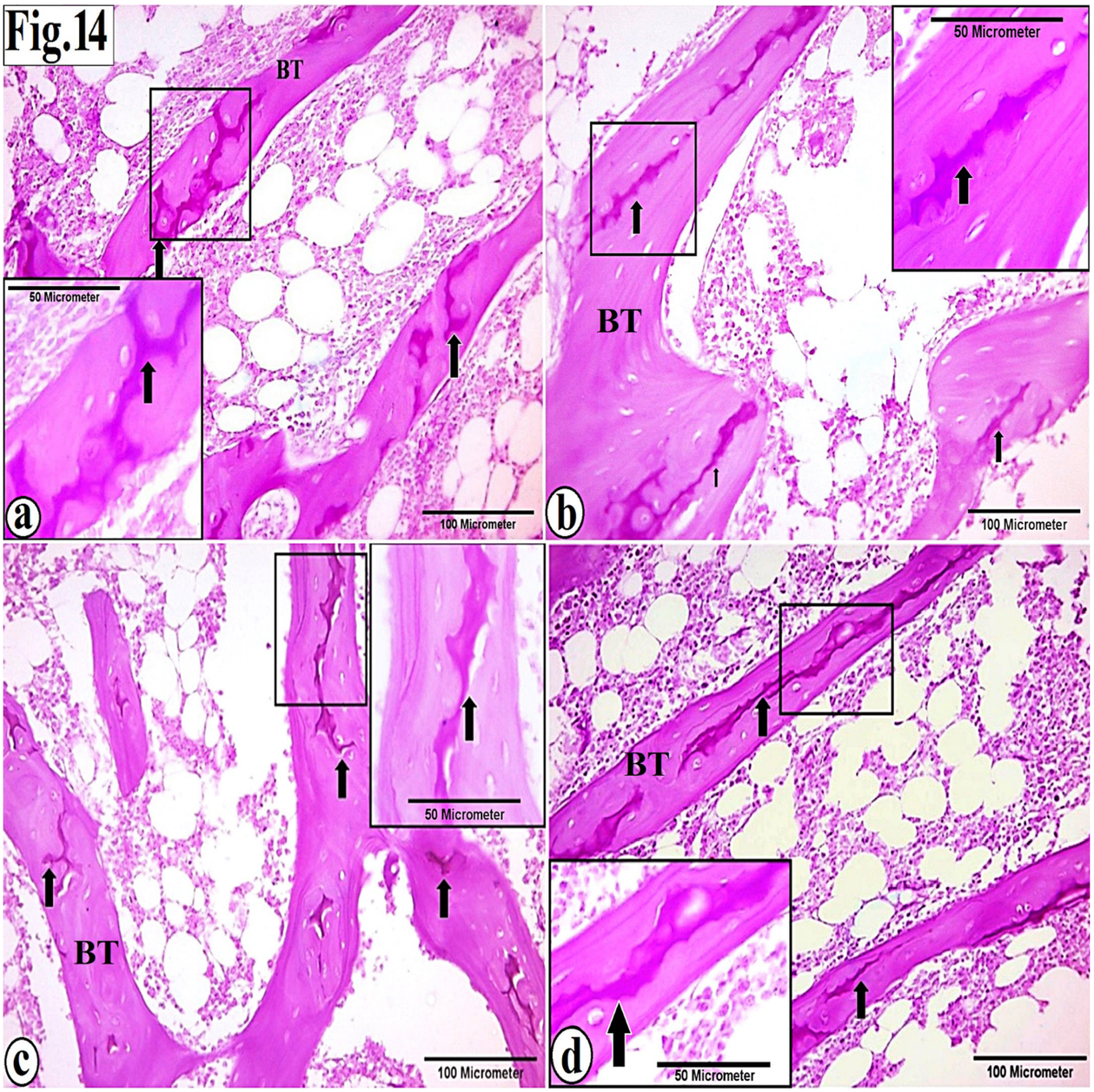

Fig. 14: Photomicrographs from the femurs' epiphyses of the treated groups: (a) GIIIb, (b) GIIIc, (c) GIIId, and (d) GIIIe, showing: intense PAS-positive reactions in the cement lines (arrows) within the spongy bone trabeculae (BT) more or less as in the control group. The insets, at higher magnifications, show the PAS-positive cement lines within the trabecular bone matrix. [PAS reaction; (a, b, c & d) x200, scale bar = 100 µm, and (insets) x400, scale bar = 50 µm].

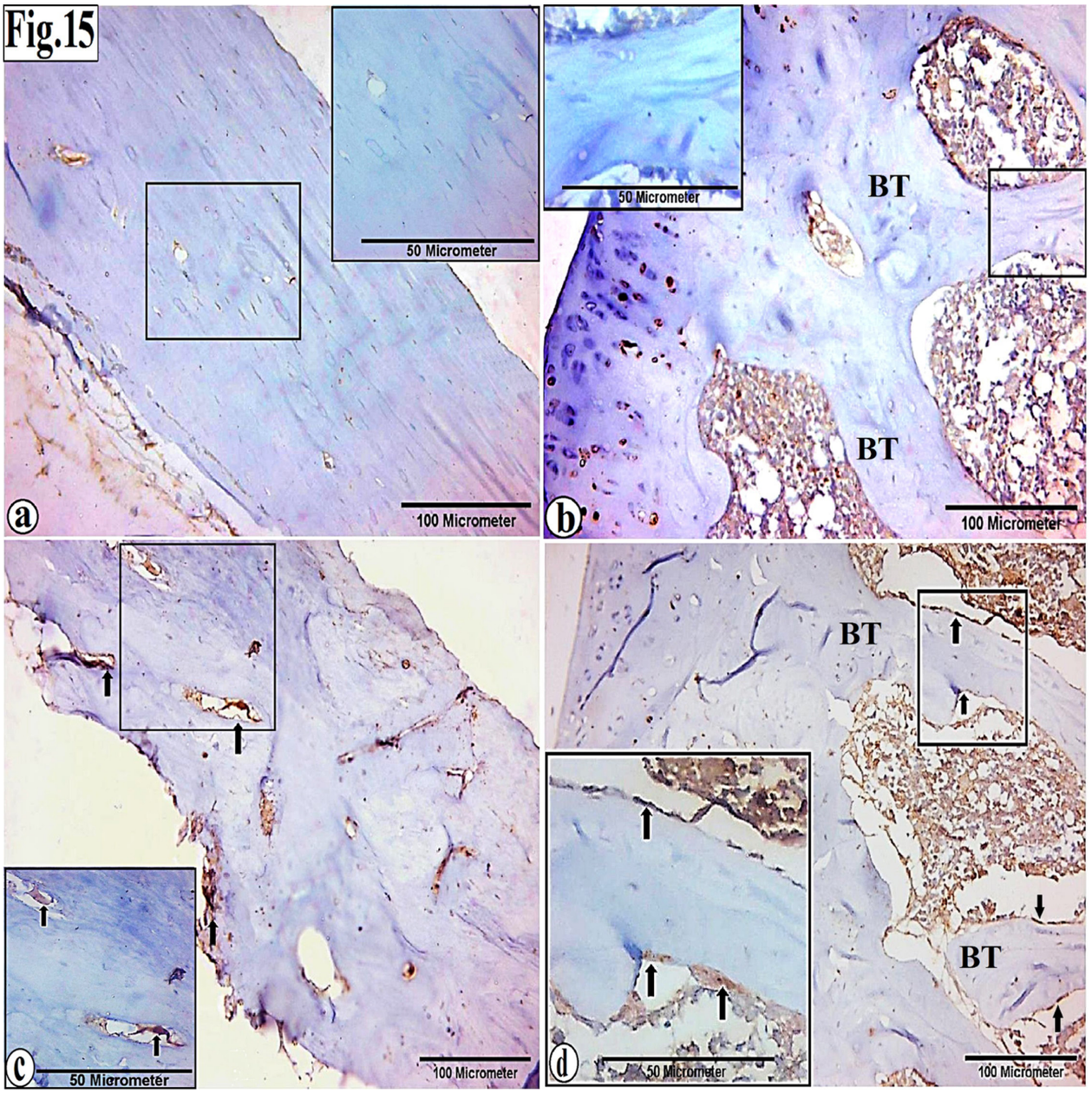

Fig. 15: Photomicrographs of sections from the femurs' shafts and epiphyses of the sham-operated and the osteoporotic groups: (a, b) Sham-operated rat (GII), showing: undetectable RANKL immune expression in the compact bone matrix and within the bone trabeculae (BT). The insets at higher magnifications show undetectable RANKL immune expression within the same regions. (c, d) The osteoporotic group (GIIIa), showing: strong positive RANKL immune expression (arrows) in the osteoporotic cavities and within the endosteum of the compact bone, as well as within the endosteum of the trabecular bone (BT). The insets, at higher magnifications, show the positive RANKL immune expression (arrows) within the osteoporotic cavities and the endosteum of the osteoporotic group. [RANKL immune expression; (a, b, c, d) x200, scale bar = 100µm, and (inset) x400, scale bar = 50 µm].

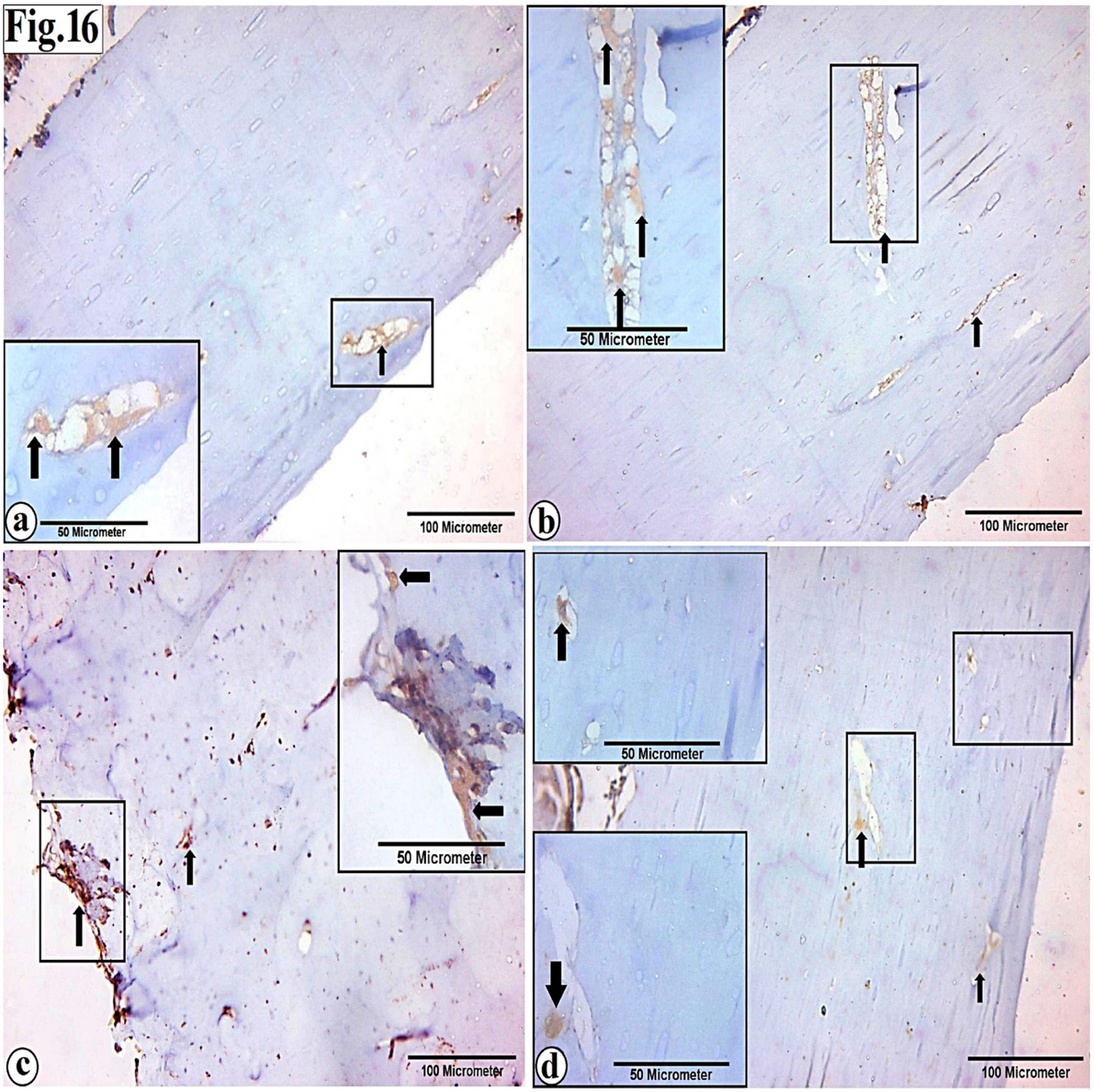

Fig. 16: Photomicrographs of sections from the femurs' shafts of the treated groups; (a) Fosamax-treated group (GIIIb), (b) Mena Q-treated group (GIIIc), and (c) Fennel-treated group (GIIId) show: mildly positive RANKL immunoexpression (arrows) in the osteoporotic cavity within the compact bone matrix and at the endosteal lining of the compact bone. (d) Mena Q and Fennel-treated group (GIIIe), demonstrating: faint RANKL immune expression (arrows) within the compact bone matrix. The insets, at higher magnifications, show the positive RANKL immune expression (arrows) in the detected regions. [RANKL immune expression; (a, b, c, d) x200, scale bar = 100µm, and (inset) x400, scale bar = 50 µm].

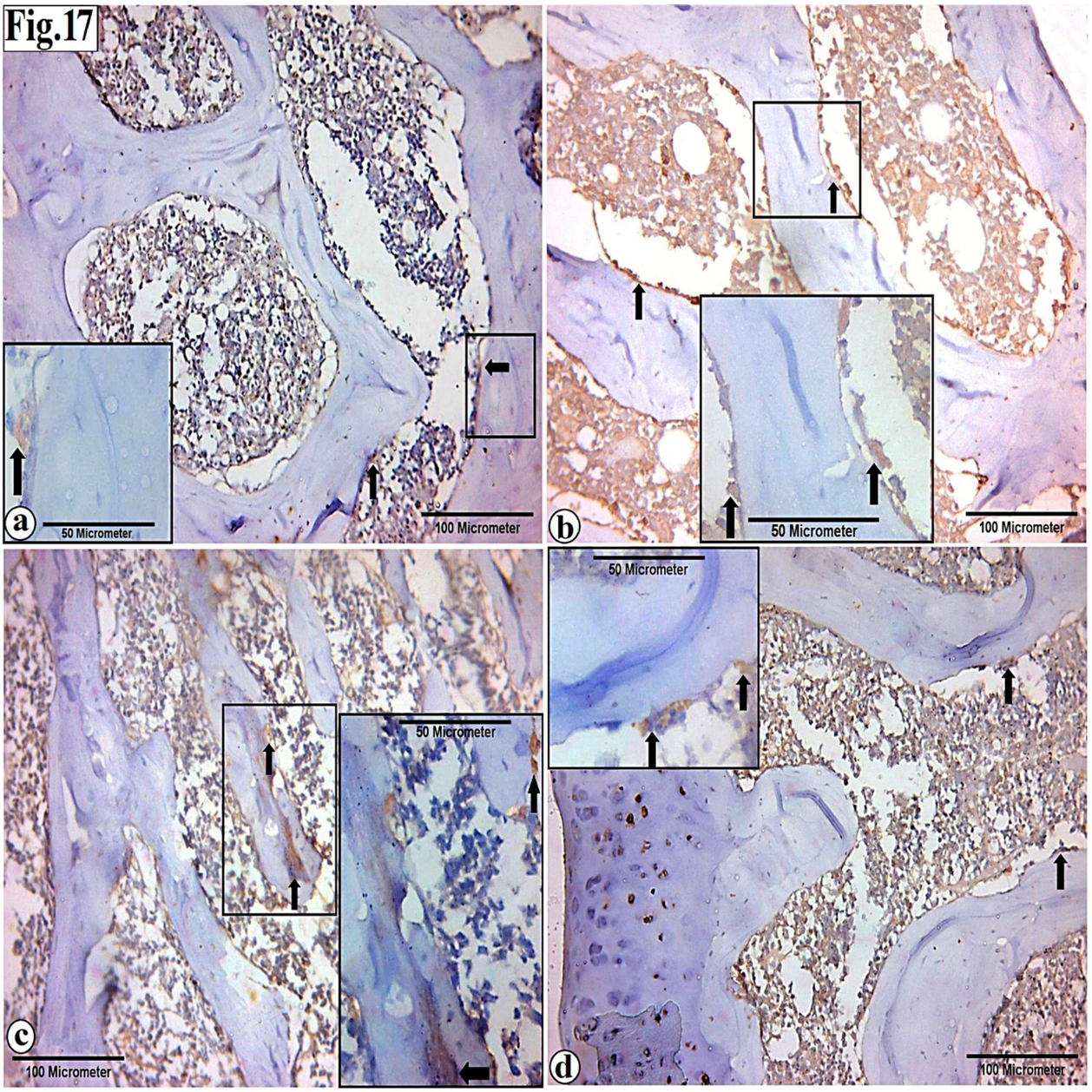

Fig. 17: Photomicrographs from the femurs' epiphyses of the treated groups (a) GIIIb, (b) GIIIc, (c) GIIId, and GIIIe, showing: faint RANKL immune expression (arrows) within the endosteum of the trabecular bone. The insets, at higher magnifications, show the positive RANKL immune expression (arrows) at the trabecular bone's endosteum. [RANKL immune expression; (a, b, c, d) x200, scale bar = 100µm, and (inset) x400, scale bar = 50 µm].

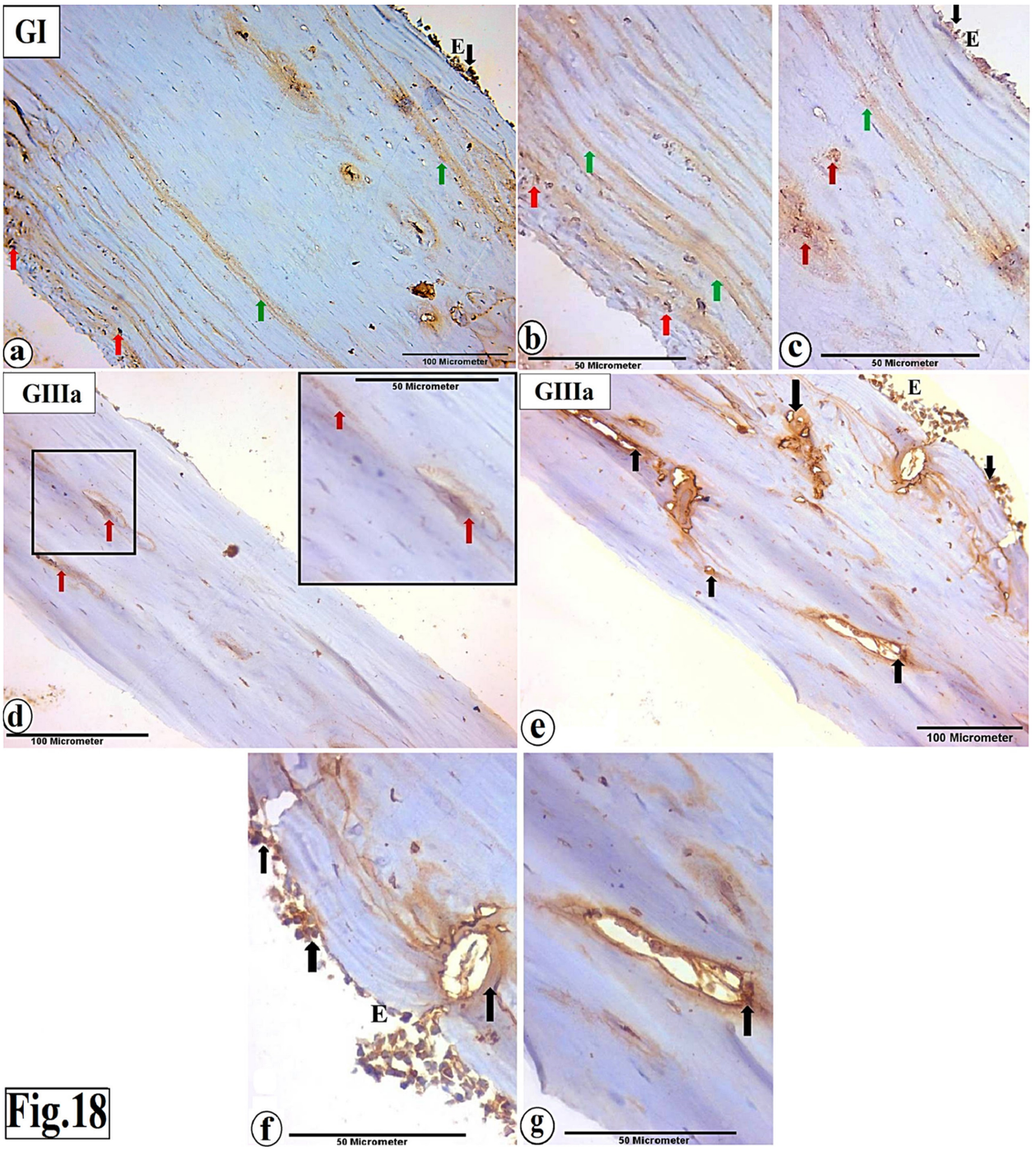

Fig.18

Fig. 18: Photomicrographs of sections from the femurs' shafts of the control and the osteoporotic groups: (a, b, c) control rats (GI), showing: positive osteopontin (OPN) brown granules in the bone matrix (red arrows), in the cement lines (green arrows), as well as at the endosteum (E) (black arrows). (d) The osteoporotic group (GIIIa) shows: a weak osteopontin immune expression within the compact bone matrix (red arrows). The inset, at a higher magnification, shows the weak OPN immune expression in the matrix of compact bone. (e, f, g) Another section from the osteoporotic group (GIIIa), shows: a strong positive OPN immune expression (black arrows) within the osteoporotic cavities and at the endosteal surface (E) of the compact bone. [OPN immune expression; (a, d, g) x200, scale bar = 100 µm, (b, c, e, f and inset in g) x400, scale bar = 50 µm].

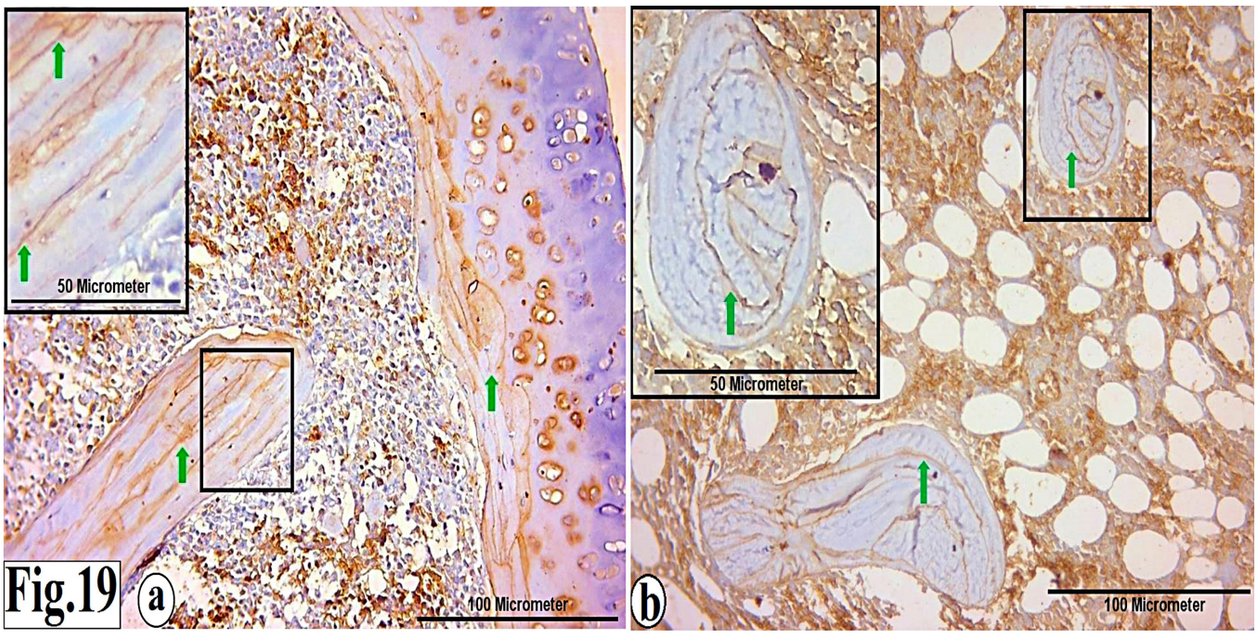

Fig. 19: Photomicrographs of sections from the epiphyses of the femurs of the control and the osteoporotic groups: (a) A control rat (GI), showing: a positive osteopontin (OPN) immune expression in the cement lines (green arrows) of the bone trabeculae. (b) The osteoporotic group (GIIIa) shows: a weak osteopontin immune expression in the cement lines of the discontinuous bone trabeculae (green arrows). The insets, at higher magnifications, show the OPN osteopontin immune expression in the detected regions. [OPN immune expression; (a, b) x200, scale bar = 100 µm, and (insets) x400, scale bar = 50 µm].

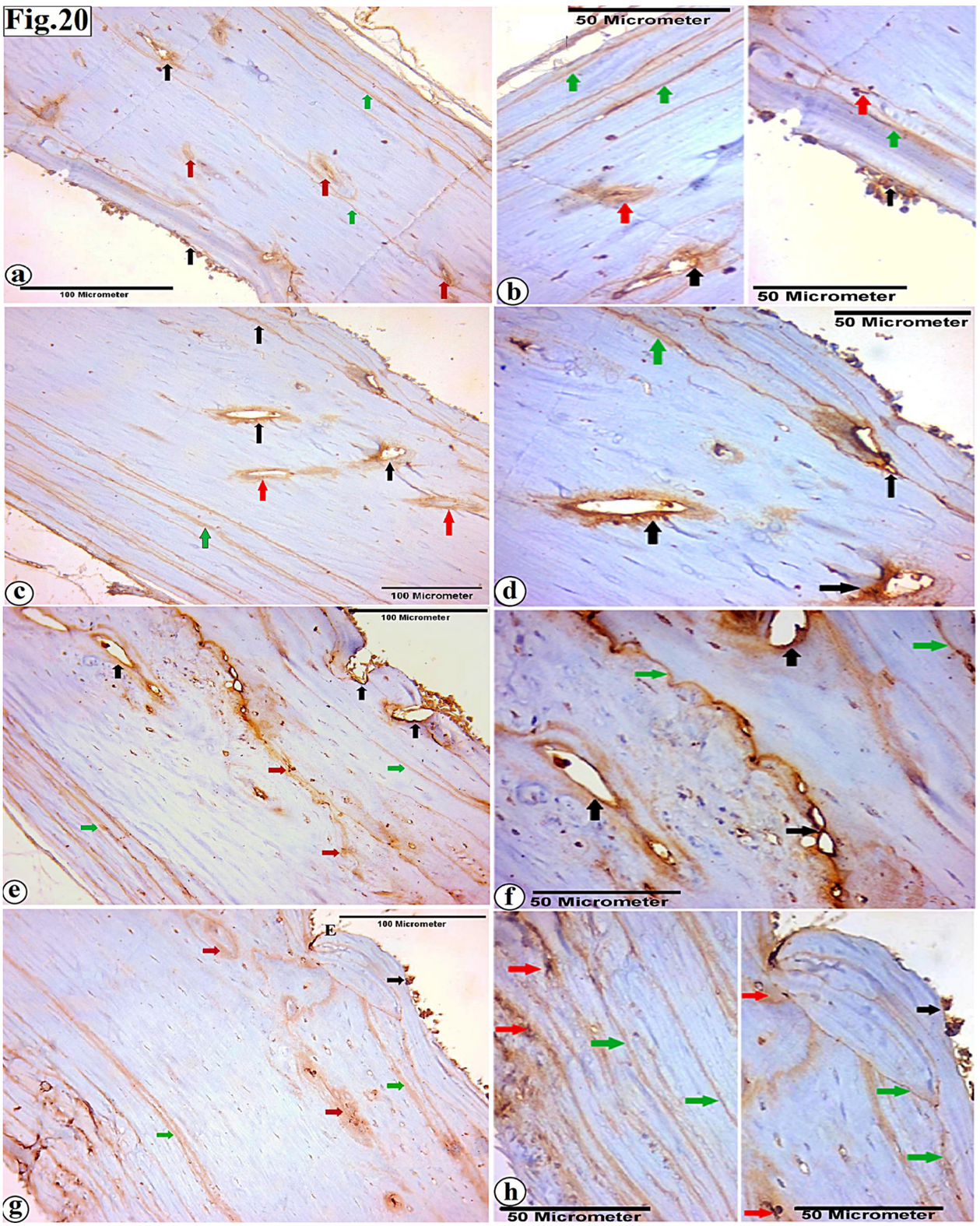

Fig. 20: Photomicrographs of sections from the femurs' shafts of the treated groups: (a, b) Fosamax-treated group (GIIIb), (c, d) Mena Q-treated group (GIIIc), (e, f) Fennel-treated group (GIIId), and (g, h) Mena Q and Fennel-treated group (GIIIe), showing: strong positive OPN immune expression in the bone matrix (red arrows), in the cement lines (green arrows), as well as at the endosteum (E) (black arrows). (b, d, f) Higher magnifications show: Strong positive OPN immune expressions (black arrows) within the osteoporotic cavities of the compact bone in GIIIb, GIIIc, and GIIId. [OPN immune expression; (a, c, e, g) x200, scale bar = 100 µm, and (b, d, f, h) x400, scale bar = 50 µm].

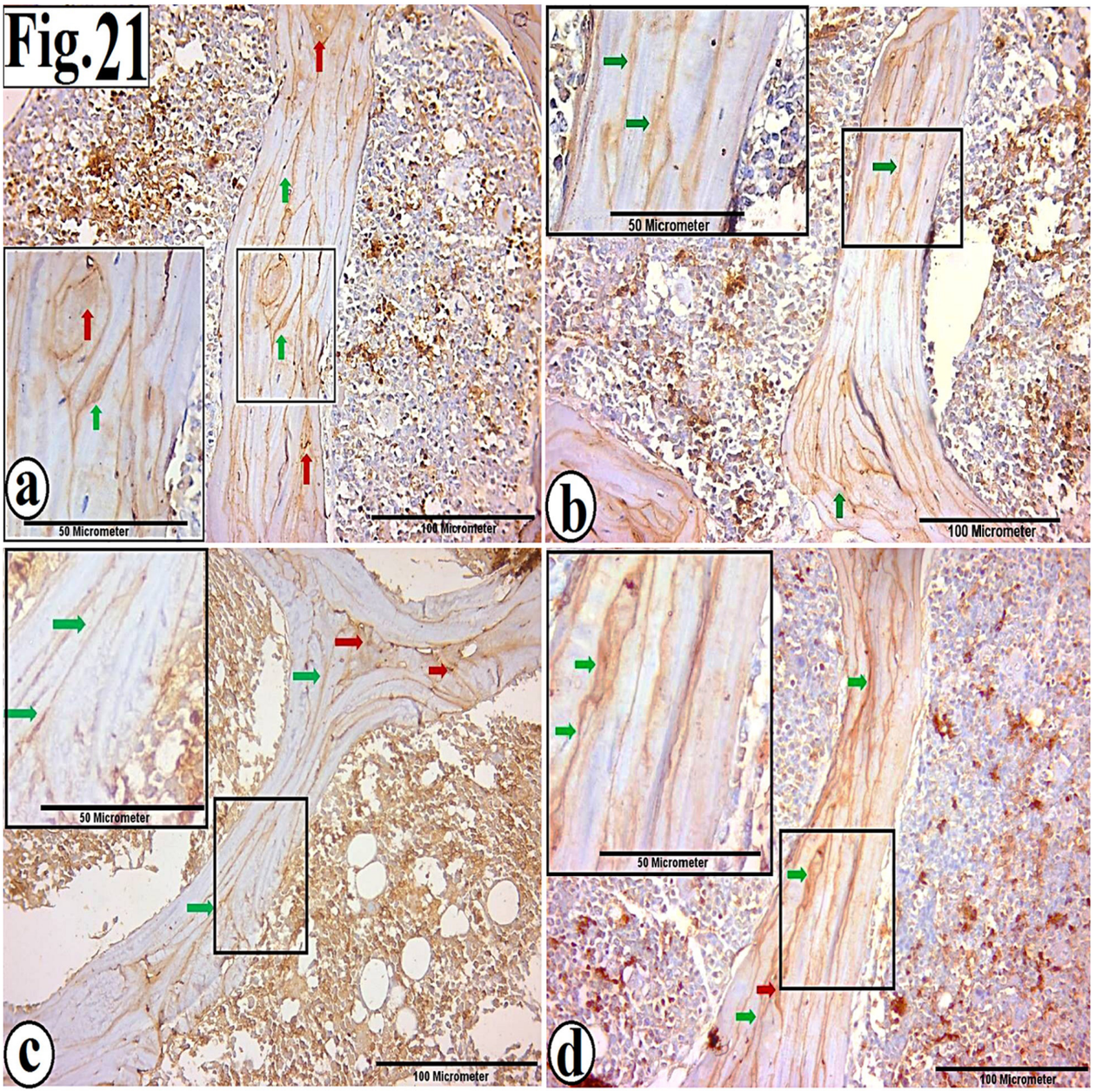

Fig. 21: Photomicrographs of sections from the femurs' epiphyses of the treated groups: (a) GIIIb, (b) GIIIc, (c) GIIId, and (d) GIIIe, showing: strong positive OPN immune expression in the cement lines (green arrows) and within the bone matrix (red arrows) of the bone trabeculae. The insets, at higher magnifications, show the OPN immune expression in the detected regions. [OPN immune expression; (a, b, c, d) x200, scale bar = 100 µm, and (insets) x400, scale bar = 50 µm].

Table 1: The mean values of initial and final body weight (g) among all the experimental groups.

Groups parameters	(Group (I N = 6	Group (II) N = 6	Group (IIIa) N = 6	Group (IIIb) N = 6	Group (IIIc) N = 6	Group (IIId) N = 6	Group (IIIe) N = 6	Test of significance	*P*
Initial body weight (g)	145.8±4.9	146.6± 6.0	146.6±6.1	150.0±3.1	147.5±2.7	148.3±4.1	152.5±5.2	ANOVA F=1.43	0.231
Final body weight (g)	230.8±8.6	233.3±9.3	305.0±11.8	260.0±7.0	259.1±5.8	250.8±7.3	241.6±5.1	ANOVA F=56.92	0.000*

Data are presented as means ± standard deviation (SD)
N = Number of animals, g = grams
* = $P \leq 0.05$ = Significant
$P > 0.05$ = Non significant
significant versus the control group (GI)
significant versus the osteoporotic group (GIIIa)
significant versus the Fosamax-treated group (GIIIb)
significant versus the MenaQ -treated group (GIIIc)

Table 2: The mean values of Calcium, Phosphorus, Bone specific alkaline phosphatase (BALP) and Tartrate-resistant acid phosphatase (TRAP) among rats of the experimental groups.

Groups parameters	(Group (I N = 6	Group (II) N = 6	Group (IIIa) N = 6	Group (IIIb) N = 6	Group (IIIc) N = 6	Group (IIId) N = 6	Group (IIIe) N = 6	Test of significance	*P*
Calcium (mg/dl):	10.9±1.0	10.1±0.6	3.8± 0.4	8.4± 0.1	7.9±0.2	6.8±0.7	9.2±1.0	ANOVA F=99.62	0.000*
Phosphorus (mg/dl):	18.9±0.4	18.3±0.3	12.8±1.2	15.1±3.1	14.8±2.5	14.7±0.9	17.8±1.9	ANOVA F=10.01	0.000*
Bone ALP (IU/L):	64.0±1.1	66.1±1.5	130.9±8.6	77.9±3.8	84.0±2.4	100.1±8.3	66.8±1.7	ANOVA F=26.21	0.000*
TRAB-5b (ng/ml):	0.42±0.03	0.45±0.02	3.1±0.04	0.54±0.02	0.76±0.01	0.83±0.04	0.51±0.03	ANOVA F=97.68	0.000*

Data are presented as means ± standard deviation (SD)
N = Number of animals
* = $P \leq 0.05$ = Significant
$P > 0.05$ = Non significant
significant versus the control group (GI)
significant versus the osteoporotic group (GIIIa)
significant versus the Fosamax-treated group (GIIIb)
significant versus the MenaQ -treated group (GIIIc)
significant versus Fennel -treated group (GIIId)

Table 3: The mean values of osteocyte number, cortical thickness (µm), area percentage (%) of the trabecular thickness, and the epiphyseal plate thickness (µm) among rats of the experimental groups

Groups parameters	(Group (I N = 6	Group (II) N = 6	Group (IIIa) N = 6	Group (IIIb) N = 6	Group (IIIc) N = 6	Group (IIId) N = 6	Group (IIIe) N = 6	Test of significance	P
Osteocyte Count	150.3±7.7	148.0±11.5	66.5±6.3	119.5±7.2	110.5±5.9	89.5±4.6	130.3±5.5	ANOVA F=104.48	0.000*
Cortical Thickness (µm)	426.3±7.0	425.6±5.5	215.0±6.2	392.1±5.7	371.3±5.6	353.9±7.3	411.4±5.3	ANOVA F=866.24	0.000*
Area % of the trabecular thickness	64.1±3.0	62.6±3.6	23.7±2.2	49.3±3.8	45.9±3.4	41.8±1.5	59.7±2.9	ANOVA F=130.98	0.000*
Epiphyseal plate thickness (µm)	258.5±7.5	254.9± 9.3	69.6±4.9	231.9±5.5	199.8±4.2	176.2±7.6	242.1±5.1	ANOVA F=559.1	0.000*

Data are presented as means ± standard deviation (SD)
N = Number of animals, µm = Micrometer
* = $P \leq 0.05$ = Significant
$P > 0.05$ = Non significant
significant versus the control group (GI)
significant versus the osteoporotic group (GIIIa)
significant versus the Fosamax-treated group (GIIIb)
significant versus the MenaQ -treated group (GIIIc)
significant versus Fennel -treated group (GIIId)

Table 4: The mean area percentage (%) of collagen fibers in the shaft and the trabeculae, and the mean PAS-Optical density in shaft and the trabeculae among rats of the experimental groups

Groups parameters	Group (I) N = 6	Group (II) N = 6	Group (IIIa) N = 6	Group (IIIb) N = 6	Group (IIIc) N = 6	Group (IIId) N = 6	Group (IIIe) N = 6	Test of significance	*P*
Area % of collagen fibers in the shaft	40.48±3.34	40.02±3.35	8.27±1.04	39.28±1.34	37.27±4.28	34.83±1.42	39.40±2.61	ANOVA F=107.60	0.000*
Area % of collagen fibers in the trabeculae	34.81±1.62	34.11±2.02	8.01±0.93	28.84±2.84	27.99±0.99	25.46±1.77	29.88±2.51	ANOVA F=140.25	0.000*
PAS-Optical density in shaft	0.59±0.03	0.58±0.01	0.28±0.01	0.73±0.04	0.68±0.06	0.54±0.03	0.79±0.06	ANOVA F=76.99	0.000*
PAS-Optical density in trabeculae	0.53±0.05	0.51±0.03	0.31±0.04	0.65±0.01	0.59±0.02	0.50±0.02	0.65±0.04	ANOVA F=60.30	0.000*

Data are presented as means ± standard deviation (SD)
N = Number of animals
* = $P \leq 0.05$ = Significant
$P > 0.05$ = Non significant
significant versus the control group (GI)
significant versus the osteoporotic group (GIIIa)
significant versus the Fosamax-treated group (GIIIb)
significant versus the MenaQ -treated group (GIIIc)
significant versus Fennel -treated group (GIIId)

Table 5: The mean area percentage (%) of the RANKL and OPN immuno-expression in the cortical and the trabecular bone among rats of the experimental groups

Groups parameters	(Group (I N = 6	Group (II) N = 6	Group (IIIa) N = 6	Group (IIIb) N = 6	Group (IIIc) N = 6	Group (IIId) N = 6	Group (IIIe) N = 6	Test of significance	*P*
RANKL expression in Shaft (%)	0.38±0.07	0.46±0.06	4.41±0.57	1.16±0.33	1.55±0.50	1.85±0.33	0.67±0.11	ANOVA F=97.79	0.000*
RANKL expression in Trabeculae (%)	1.41±0.22	1.96±0.08	7.39±0.74	2.26±0.34	2.43±0.29	2.86±0.11	2.06±0.23	ANOVA F=193.95	0.000*
OPN expression in shaft (%)	20.58±1.23	20.19±0.9	15.86±1.03	17.28±0.83	16.82±1.27	16.42±0.65	18.28±0.9	ANOVA F=20.47	*P*=0.000*
OPN expression in trabeculae (%)	11.82±0.61	11.19±0.76	8.6±0.97	10.18±0.84	9.66±0.71	9.14±1.8	10.63±1.0	ANOVA F=130.98	*P*=0.000*

Data are presented as means ± standard deviation (SD)
N = Number of animals.
* = $P \leq 0.05$ = Significant
$P > 0.05$ = Non significant
significant versus the control group (GI)
significant versus the osteoporotic group (GIIIa)
significant versus the Fosamax-treated group (GIIIb)
significant versus the MenaQ -treated group (GIIIc)
significant versus Fennel -treated group (GIIId)

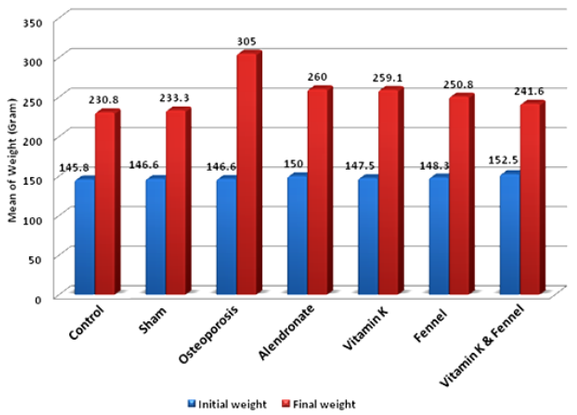

Histogram 1: The mean value of initial and final weight among all experimental groups

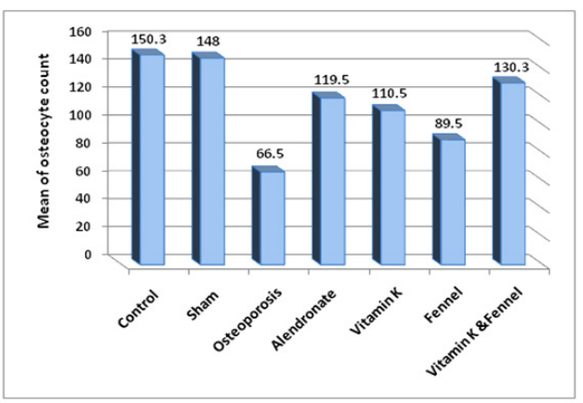

Histogram 2: The mean value of osteocyte count among all experimental groups

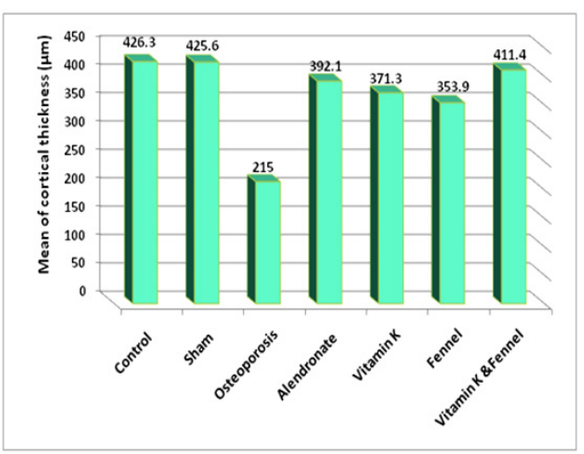

Histogram 3: The mean cortical thickness (µm) of the shaft among all experimental groups

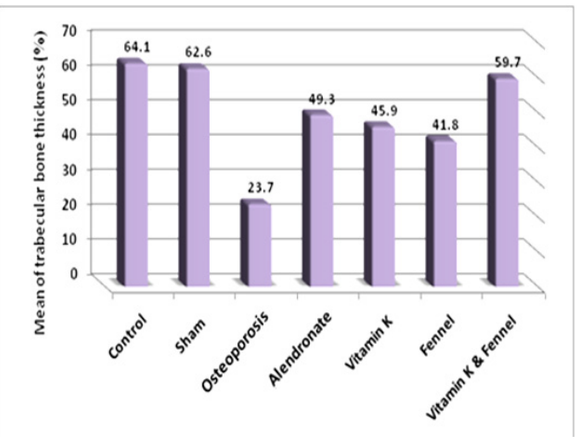

Histogram 4: The mean area percentage of the trabecular bone thickness among all experimental groups

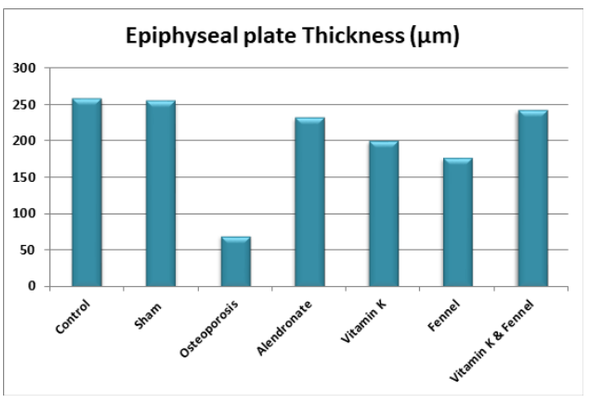

Histogram 5: The mean thickness of epiphyseal growth plate cartilage (µm)among all experimental groups

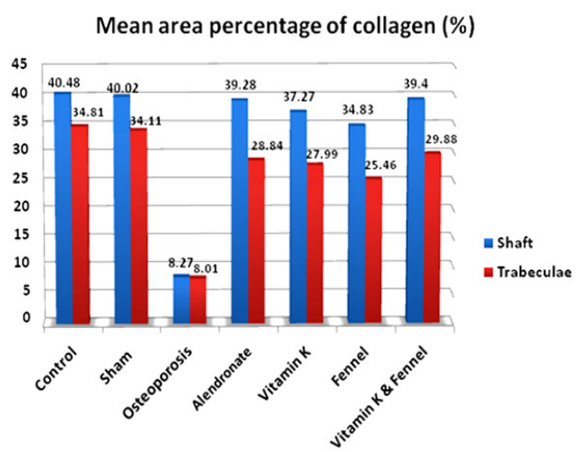

Histogram 6: The mean area percentage of collagen fibers in the cortical and trabecular bone among all experimental groups

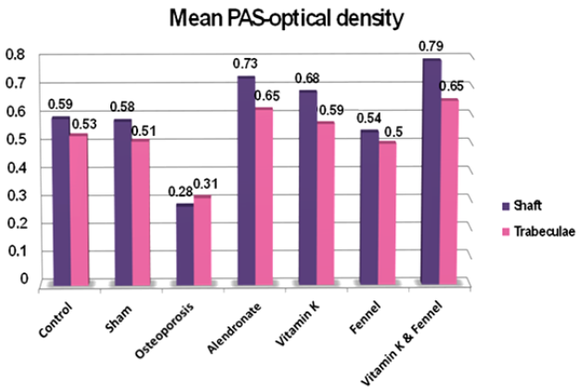

Histogram 7: The mean optical denisty of PAS-positive cement ground matrix in the cortical and the trabecular bone among all experimental groups

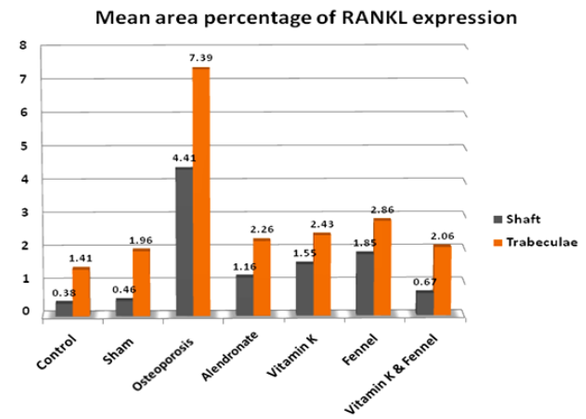

Histogram 8: The mean area percentage (%) of the RANKL expression in the cortical and the trabecular bone among all experimental groups

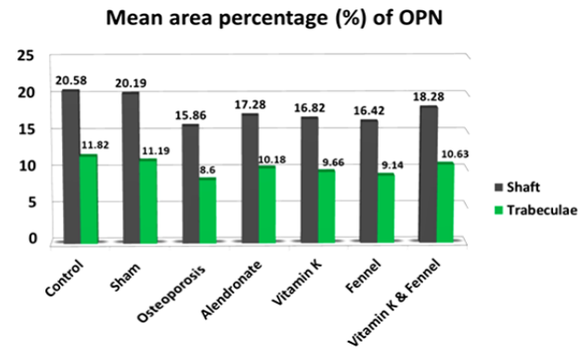

Histogram 9: The mean area percentage (%) of the OPN expression in the cortical and in the trabecular bone among all experimental groups

DISCUSSION

Osteoporosis is a serious health issue among postmenopausal females linked to ovarian hormonal deficiency. An imbalance between bone formation and resorption, as well as an increase in bone turnover, leads to rapid bone loss. As a result, most postmenopausal women have an increased risk of fracture[2,22].

Fosamax (Alendronic acid) is one of the most popular drugs widely used in the treatment of osteoporosis because it is a nitrogen-containing bisphosphonate that stimulates the proliferation of preosteoblasts and the apoptosis of osteoclasts[5,23].

Medical services experts are very interested in Mena Q, a highly purified long-acting form of vitamin K2, for its possible potential benefits on human health as it promotes osteoblast proliferation and differentiation while inducing apoptosis in osteoclasts[6].

Fennel essential oil has attracted the attention of consumers and healthcare professionals for its potential effects on human well-being due to its antioxidant properties and natural estrogenic activity[7].

The current study aimed to assess the effects of Fosamax, Mena Q, and Fennel essential oil on changes that occurred as a result of postmenopausal (ovariectomy) osteoporosis. These alterations include body weight gain, serum calcium, phosphorous, BALP, and TRAP levels, as well as the histological structure of the femur in adult female albino rats.

The animal doses for Fosamax, 0.2 mg/ml/rat once a week, and Mena Q, 0.5 mg/ml/rat once daily, were calculated from the human doses of 70 mg/adult human being[10] and 1 g/adult human being[11], respectively. The study by Kim *et al*.[12] found that fennel essential oil at a dose of 1 ml/day/rat was equivalent to 100 mg/kg body weight of a human being.

The drugs used in the current study were introduced via an oro-gastric tube to ensure that the animal consumed the exact dose of the medications[7].

Ovariectomy in female rats causes menopause-like symptoms and exhibits the same hormonal changes as seen in humans with osteoporosis[7]. This provides a useful way to study the pathophysiology of the distinctive metabolic and reproductive disorders and consequently find novel and effective treatments[24].

Studies about the time needed for osteoporosis to develop following experimental menopause were controversial. According to Liu *et al*.[13] and Rajfer *et al*.[14], osteoporosis occurred twelve weeks after ovariectomy. Nevertheless, Zheng *et al*.[25] reported that it occurred fifty days following an ovariectomy. In the current study's pilot experiment, postmenopausal osteoporosis was proven twelve weeks following ovariectomy.

In the present study, the increased body weight was a well-documented observation in the osteoporotic group (GIIIa), which could be related to the disturbance of the gut hormones that regulate satiety, such as ghrelin and adiponectin, and the occurrence of neural leptin resistance as a result of ovarian hormones withdrawal[26], with subsequent increasing local cortisol concentrations and declining thyroid gland activities, followed by sleep deprivation, exhaustion, and diminishing motor activity, which may end in postmenopausal obesity[27,28].

As post-menopausal women lack ovarian hormone production with a decline in systemic estrogen levels, the gut microbiome may be altered and the enterohepatic recycling of hormones may be disturbed, which are linked to substantial changes in metabolic health[29].

The osteoporotic group (GIIIa) had lower serum calcium and phosphorus levels coupled with significantly higher levels of bone-specific alkaline phosphatase (BALP) and tartrate-resistant acid phosphatase (TRAP-5b) when compared to the control group. According to Bhadarge *et al*.[4] and Shakoor *et al*.[30], reformist withdrawal of estrogen in postmenopausal women is linked to diminished calcium absorption by intestinal microvilli and increased calcium excretion from the aging kidney. Lowering serum calcium levels reduces the kidney's ability to produce 1, 25-dihydroxy vitamin D, which causes secondary hyperparathyroidism and, in turn, prompts osteoclasts to resorb bone.

Additionally, reducing 1, 25 dihydroxy vitamin D decreases phosphorous absorption by the intestinal villi and reduces phosphorous renal reabsorption, which could have an undesirable effect on bone mineral content[4,30].

The increase in BALP and TRAP levels seen in GIIIa was consistent with the findings of Pardhe *et al*.[31] and Gurban *et al*.[32], who stated that BALP and TRAP5b are the most specific markers of bone turnover, and their high levels in postmenopausal females are therefore attributed to the loss of estrogen's inhibitory effect on the process of bone resorption. Only osteoblasts produce BALP, exclusively a glycoprotein that enhances the mineralization process by degrading pyrophosphate-based mineralization inhibitors at an alkaline pH and providing a high phosphate concentration at the osteoblastic surface. However, the mechanism by which BALP affects bone mineralization is still poorly understood.

TRAP 5b, an osteoclast-specific product typically released into the region between the osteoclasts' ruffled border and the endosteum during bone resorption, dephosphorylates numerous bone matrix proteins, including osteopontin and sialoprotein, which increases bone resorption. Therefore, states of high bone turnover were linked to a higher TRAP5b level, which correlates with both the quantity and activity of osteoclasts[32,33].

The femur was chosen in the current study as it is the longest and strongest bone in the body and is easy to remove from rats and process for histological examination to examine both types of bone: compact bone in the shaft and spongy bone in the epiphysis[34].

The histological results in the present study were consistent with the serological results. The most obvious bone deterioration in the osteoporotic rats (GIIIa) in H&E stained sections was a significant reduction in the thickness of the shaft and bone trabeculae, and the appearance of faintly stained focal areas within the acidophilic matrix with irregular basophilic regions in between. Moreover, there were fewer osteocytes, empty lacunae, osteoporotic cavities, and substantial bony tunnels. Thin, discontinuous trabeculae with wide bone marrow spaces containing fewer hemopoietic cells and abundant adipocytes could be seen. Blind-ended trabeculae were accompanied by tiny fissures, fractures, and button-shaped islets. The endosteum revealed an unevenly eroded surface. A significant reduction in epiphyseal cartilage thickness was observed, and some chondrocytes were disorganized or even missing. These findings were confirmed by histomorphometric measurements and statistical analysis.

Reactive oxygen species (ROS) and oxidative stress are considered the main mechanisms accelerating osteoporosis in postmenopausal women. Estrogen deficiency induces an unregulated chronic, low-grade inflammatory disorder that is responsible for bone aging and deterioration of bone histoarchitecture by either reducing osteoblast proliferation with decreasing osteoblastic life span or by producing various osteoclastogenic cytokines within the bone micro¬environment such as Tumor necrosis factor alpha (TNF-α) and upregulating stromal cell production of RANKL and macrophage colony-stimulating factor (M-CSF) which induce osteoclastogenesis and osteoclast activity which in turn enhance the occurrence of a gap between bone formation and resorption, disturbs skeletal homeostasis, and dysregulates bone density[5,35].

Additionally, the irregularly arranged osteocytes, areas devoid of osteocytes, and a few empty lacunae in the current study's findings were attributed to apoptosis dysregulation of osteoblasts and osteocytes following estrogen deficiency, with severely disturbed bone matrix biosynthesis, bone mineralization, loss of osteon organization, and lamellar bone structure[36,37].

The wide bone marrow spaces between bone trabeculae containing abundant adipocytes were explained by the adipogenic transcription factors, which are expressed and activated in hematopoietic lineage cells during osteoclast differentiation and are crucial for lineage priming, differentiation, and osteoclast activity. It is well established that the differentiation programes for adipogenesis and osteoblastogenesis are competitively balanced, and as a result, increased bone marrow adipogenesis can negatively affect the mesenchymal stem cell osteoblast differentiation program, which in turn can have a negative impact on bone remodeling[37,38].

A significant decrease in the density and distribution of collagen fibers within the bone matrix of the compact bone and the bone trabeculae in GIIIa in Masson's trichrome-stained sections was mainly due to the loss of estrogen's stimulating effect on the promoters of genes involved in bone matrix biosyntheses, such as glycosaminoglycans and collagen type 1, as a consequence of menopause[25,36].

The ill-defined PAS-positive cement lines within the bone matrix that were detected in the GIIIa using the PAS technique might be due to a combination of altered cellular activities that are influenced by lower estrogen

levels in post-menopausal osteoporosis, such as increased osteoclastic intensity, shortened osteoblastic life span, and suppression of its spontaneous activity that may reduce new bone formation and subperiosteal bone deposition and may have an impact on net bone volume as well as the capacity to withstand an ideal load[39,40].

A strong RANKL immune expression in the osteoporotic cavities and within the endosteum of the femur of the GIIIa could be attributed to increased osteoclast activity as a consequence of post-menopausal osteoporosis. RANKL, an uncoupling factor secreted by the stromal osteoblast lineage cells, including osteoblasts, osteocytes, and osteoprogenitor cells, coordinates bone remodeling by binding to RANK receptor in osteoclast precursors and is involved in osteoclast differentiation and stimulation. As a result, adjacent osteoblasts are subsequently stimulated with increased RANKL secretion, which implies an increase in bone turnover related to bone fracture and structural alterations[41].

Zheng *et al*.[25]; Chen *et al*.[42] & Rajan *et al*.[43] also stated that estrogen deficiency causes an imbalance between serum osteoprotegerin (OPG)/RANKL ratio, bone OPG/RANKL mRNA expression ratio, and RANK/RANKL/OPG, which are crucial pathways in maintaining an appropriate balance between bone resorption, and bone formation and play a significant role in skeletal integrity. OPG, a naturally occurring cytokine primarily produced by the osteoblastic lineage, blocks the binding of RANKL to RANK and inhibits the osteoclast formation and activation. Thereby, the elevation of these ratios following menopause results in osteoclast activation and the occurrence of postmenopausal osteoporosis.

Osteopontin (OPN), an extracellular protein synthesized by fibroblasts and cells of the osteoblastic lineage, binds tightly to hydroxyapatite crystals in the bone matrix along with type I collagen bundles, forming an integral part of the mineralized matrix. Hydroxyapatite crystals are also expressed between the processes of osteoclasts' ruffled borders. As a result, positive OPN reactions normally appear in the vicinity of osteoblasts and osteocytes, in the cement lines (newly formed bone), and at the endosteum[22,36,44].

In the present study, a weak osteopontin immune reactivity within the bone matrix in both shaft and trabecular bone of the osteoporotic group's femur (GIIIa) might be attributed to the postmenopausal estrogen deficiency, which may dysregulate OPN expression through estrogen receptor alpha (ERα) and/or ERRα-mRNA, either independently or in combination, although the mechanisms are still unclear[36,45].

On the contrary, strong positive OPN reactions detected in the osteoporotic cavities and at the endosteal surface in GIIIa were consistent with Baloğlu and Gökalp-Özkorkmaz[24] and Liu *et al*.[41]. They stated that OPN is a versatile multifunctional protein important in osteoblastogenesis and osteoclastogenesis and plays a vital role in bone formation or resorption according to the function of the cells linked to the particle matrix. OPN activation in osteoblasts may quicken the osteoclasts' adhesion and activation, thereby enhancing bone resorption, although the dual mechanism remains uncertain.

In the current study, the groups treated with Fosamax (GIIIb), Mena Q (GIIIc), and fennel (GIIId) all demonstrated improvements in body weight and serological parameters, with significantly increased serum calcium and phosphorous levels coupled with a significant reduction in BALP and TRAP-5 levels indicating a decrease in the bone turnover process. The best results were recorded among the Mena Q and fennel-treated group (GIIIe).

The precise mechanism by which vitamin K affects body weight is still controversial. Regular menaquinone (MK) supplementation, one of the vitamin K forms, may reduce total fat accumulation and serum triglycerides in rats by improving osteocalcin carboxylation and increasing the insulin sensitivity index, suggesting a beneficial impact of vitamin K on fat and glucose metabolism and thereby preventing postmenopausal weight gain in rats. However, it is unclear if the findings can be extrapolated to humans[46,47].

Fennel's association with weight control in the fennel-treated group (GIIId) and in GIIIe can be attributed to the trypsin inhibitors, which decrease food intake, stimulate cholecystokinin release, and enhance fat utilization as an energy source. Additionally, the trans-anethole and phenolic compounds in fennel essential oil have some estrogenic activity that indirectly improves hepatic and pancreatic glucose metabolism, regulates fat metabolism[7], and affects the serotonergic system by preventing the re-uptake of serotonin and thereby raising the serotonin levels in synaptic clefts, which increases satiety and has a reputation as an appetite suppressant. These aspects, combined with its natural diuretic effect, make fennel a great remedy for promoting weight loss[48,49].

Improved serum calcium, phosphorous, BALP, and TRAP5b levels in rats of the Fosamax-treated group (GIIIb) were in accordance with Gurban *et al*.[32] & Bellido and Plotiken[50], who stated that alendronate is a potential anabolic factor for bone tissue as well as a potent inhibitor of osteoclast-mediated bone resorption by direct osteoclast apoptotic effect and preventing osteoblast and osteocyte apoptosis, thus reducing BALP and TRAP5b levels and primarily increasing renal tubular reabsorption of Ca2+ and phosphorous from the glomerular filtrate.

The improvement that was recorded in the Mena Q-treated group (GIIIc) and in GIIIe may be related to the potent antioxidative properties of vitamin K, which may improve the intestinal Ca2+ absorption across the brush border membranes of enterocytes through epithelial Ca2+ channels, potentiate protein expression and/or activate molecules involved in the transcellular and/or paracellular Ca2+ pathways such as Calbindin-28 kDa, and enhance calcium transport by the plasma membrane Ca2+ ATPase

pump or sodium-calcium exchanger, thereby improving the calcium and phosphorous levels[51].

Ahmed *et al*.[8] attributed the improvement in these biomarkers in the fennel-treated group (GIIId) and in GIIIe to the bone-sparing properties of fennel essential oil as a result of powerful antioxidant activity and the strong estrogenic activity of phytoestrogen components such as anol or dimethylated anethole, which mitigate osteoclast differentiation and function and protect osteoblasts from oxidative stress-induced apoptosis.

Interestingly, the current microscopic study revealed preservation of the normal bone histoarchitecture in all treated groups (GIIIb, GIIIc, GIIId, and GIIIe), with some basophilic areas and irregular basophilic cement lines in the femur's shaft and epiphysis indicating new bone formation. However, there were few osteoporotic cavities within the bone matrix and slight erosions in the endosteum. Compared to the osteoporotic group (GIIIa), the epiphyseal cartilage had improved, with some homogeneous regions devoid of chondrocytes.

In sections stained with Masson's trichrome and PAS, the treated groups displayed increased collagen fiber distribution within the bone matrix and an intense PAS-positive reaction with a distinctive magenta color indicative of newly formed bone in the compact bone and cancellous bone trabeculae, respectively. Kalleny[39] and Sharaf *et al*.[40] explained similar results by the fact that the newly formed collagen in the bone matrix is collagen type III, which is the emergency type, and a good candidate for repairing bone matrix, which will be replaced by the more robust and permanent collagen type I from osteoblasts, which plays a crucial role in binding calcium alongside the bone matrix with extremely strong cross-links osteocollagenous bundles, allowing more strength and stability for the newly formed bone and preventing the loss of bone mineral density.

Additionally, all treated groups revealed a weak RANKL immune expression in the osteoporotic cavities and within the endosteum, as well as a positive OPN expression in the osteoporotic cavities, within the bone matrix, and in the cement lines of the femur's shaft and trabeculae in comparison to the osteoporotic group (GIIIa). Improvement was most evident in the combined Mena Q and fennel-treated group (GIIIe). All these findings were supported by histomorphometric and statistical measurements.

Improvement in the histological structure of bone tissue that was encountered in the Fosamax- treated rats (GIIIb) could be explained by the fact that Fosamax is a nitrogen-containing bisphosphonate which has a faster and more complete removal from the bloodstream, a higher bone reattachment rate that binds more strongly to bone mineral and exerts a direct osteoclast apoptotic effect via inhibiting the enzyme farnesyl pyro phosphatases (FPPs), the key enzyme of the mevalonate pathway blocks protein prenylation, which is necessary for osteoclast survival and function, thereby inhibiting resorption of bone and increasing mineral density in bone matrix and reducing fracture risks making it a valuable first-line agent of choice in the treatment of postmenopausal osteoporosis[2,5].

Ma *et al*.[52] and Ukon *et al*.[53] stated that bisphosphonates are able to decrease bone resorption not only through their direct osteoclast apoptotic effect but also by markedly promoting the mRNA expression levels of essential transcription factors for osteoblast differentiation such as osteocalcin, osterix, and Runt-related transcription factor 2 (Runx2). As well, bisphosphonates may increase osteoblasts' production of the anti-resorptive protein osteoprotegerin and temporarily stimulate the proliferation and differentiation of preosteoblasts, inevitably preventing osteoblast and osteocyte apoptosis[22]. In conjunction with the previous effects described, this would work synergistically to reduce bone resorption.

The improvement in the Mena Q-treated group (GIIIc) and in GIIIe could be attributed to the Menaquinone-7 content, a highly purified long-acting form of vitamin K2, which has an anabolic role in bone by upregulating transcription of specific genes in osteoblasts and preventing osteoblast apoptosis, as well as promoting mesenchymal stem cell proliferation and differentiation into osteoblasts, not adipocytes, and increasing osteoblast activity[6,54].

Simes *et al*.[51] added that Mena Q assists in building and maintaining bones via activating the bone-associated vitamin K-dependent matrix Gla-protein (MGP) and calcium-bound proteins, such as osteocalcin, enhancing proper extracellular bone matrix mineralization with calcium deposition in bone, not in blood vessels. Nevertheless, The exact mechanism of action, is not well understood.

Moreover, vitamin K has antioxidative properties, protecting phospholipid membranes from peroxidation, and inhibiting I kappa B kinase (IKB) α/β phosphorylation, with a consequent decrease in the expression of several pro-inflammatory cytokines, including TNF-α, which prevents osteoblast apoptosis, potentiates osteoblast activation, and promotes 1, 25 dihydroxy vitamin D3 -induced mineralization by osteoblast-like cells. As a result, Mena Q has a predominant therapeutic effect on involutional osteoporosis[51,55].

Furthermore, Dos Santos *et al*.[46] declared that vitamin K2 prevented the osteoclast differentiation factor (ODF) / RANKL expression, a membrane surface molecule necessary for the osteoclasts' survival, development, and differentiation, thereby inhibiting osteoclastogenesis and inducing osteoclast apoptosis.

The improvement detected in the bone sections of the fennel oil-consuming rats (GIIId) and in GIIIe might be attributed to the potent estrogenic effect of phytoestrogen that resembles stilbene and diethylstilbestrol and the powerful antioxidants in fennel essential oil, such as anethole, d-limonene, beta-myrcene, and flavonoids with the highest

superoxide radical scavenging activity which protect osteoblasts from oxidative stress-induced apoptosis[7], and repress of pro-osteoclastic cytokines in osteoblasts via inhibition of nuclear transcription factor-Kappa-B (NF-κB) pathway, as well as decrease osteoclast activity on the bone surface, attenuates estrogen-dependent bone loss, and has a positive impact on matrix mineralization and bone-forming cell proliferation and ameliorating the associated biomechanical deterioration in a dose-dependent manner and thus eliminates postmenopausal osteoporosis[6,8].

Marked improvement in the bone histoarchitecture in GIIIe may be related to the synergistic antioxidant and anti-inflammatory properties of both Mena Q and fennel essential oil, as well as the flavonoids and phytosterol contents in fennel with hormone-like structures that may bind to estrogen receptor alpha and beta (ERα and ERβ) and exert estrogen-mediated suppression of osteoclasts via the regulation of the OPG/RANKL ratio, leading to a net increase in bone building and maintaining bone mineral density[6,51].

CONCLUSION AND RECOMMENDATION

The present study has generated evidence that using fennel essential oil in combination with Mena Q may be able to bring a safer and more effective treatment that may better help the body manage postmenopausal osteoporosis with preservation of the normal bone histoarchitecture and may provide a new therapeutic strategy to substitute or reduce the need for the currently-available oral synthetic drugs such as Fosamax due to the synergistic antioxidant and anti-inflammatory properties of both in addition to the potent estrogenic effect of fennel. The exact mechanism behind the therapeutic effects of fennel essential oil and Mena Q in osteoporosis remains unclear, and further research is still required to study the impact of repeated use of different amounts and forms of both agents to avoid any possible undesirable effects if they are found.

CONFLICT OF INTERESTS

There are no conflicts of interest.

REFERENCES

1. Elbahnasawy AS, Valeeva ER, El-Sayed EM and Rakhimov II. The Impact of Thyme and Rosemary on Prevention of Osteoporosis in Rats. Hindawi Journal of Nutrition and Metabolism. 2019; 10 (1155). Article 1431384:1-10. DOI:10.1155/2019/1431384.
2. Cheng CH, Chen LR and Chen KH. Osteoporosis Due to Hormone Imbalance: An Overview of the Effects of Estrogen Deficiency and Glucocorticoid Overuse on Bone Turnover. Internal Journal of Molecular Sciences. 2022; 23 (3). Article 1376:1-17. DOI: 10.3390/ijms23031376.
3. Rahimikian F, Rahimi R, Golzareh P, Bekhradi R and Mehran A. Effect of Foeniculumvulgare Mill, (Fennel) on menopausal symptoms in postmenopausal women. Menopause. 2017; 24 (9): 1017-1021. DOI: 10.1097/GME.0000000000000881.
4. Bhadarge G, Badade ZG and Kadam R. Study of calcium, phosphorous and acid phosphatase in pre and postmenopausal women. International Journal of Medical and Biomedical Studies. 2020; 4 (5): 32-35. DOI: 10.32553/ijmbs.v4i5.1114.
5. Tonk CH, Shoushrah SH, Babczyk P, El Khaldi-Hansen B, Schulze M, Herten M and Tobiasch E. Therapeutic Treatments for Osteoporosis—Which Combination of Pills Is the Best among the Bad? International Journal of Molecular Sciences. 2022; 23 (3): Article 1393: 1-36. DOI: 10.3390/ijms23031393.
6. Alonso N, Meinitzer A, Fritz-Petrin E, Enko D and Herrmann M. Role of Vitamin K in Bone and Muscle Metabolism. Calcified Tissue International. 2022; 112 (2):178–196. DOI: 10.1007/s00223-022-00955-3.
7. Sorour HA, Abdel Aal FS and Abd Elglil MM. Ovarian cytoarchitectural changes following fennel ingestion in senile diabetic albino rat. Egyptian journal of Histology. 2017; 40 (4): 427-442. DOI: 10.21608/EJH.2017.5685.
8. Ahmed AF, Shi M, Liu C and Kang W. Comparative analysis of antioxidant activities of essential oils and extracts of fennel (Foeniculum vulgare Mill.) seeds fromEgypt and China. Food Sci. Hum. Wellness. 2019; 8 (2019):67-72. https://doi.org/10.1016/j.fshw.2019.03.004.
9. Khanna V, Gupta P, Khanna R and Khanna HC. Postmenopausal Osteoporosis. Juniper Online Journal of Case Studies. 2017; 1 (4): Article 555570: 1-5. DOI: 10.19080/JOJCS.2016.01.555570.
10. Tu KN, Lie JD, Wan CK, Cameron M, Austel AG, Nguyen JK, Van K and Hyun D. Osteoporosis: A Review of Treatment Options. Pharmacy and Therapeutics. 2018; 43 (2): 92- 104. PMID: 29386866; PMCID: PMC5768298.
11. Akbulut AC, Pavlic A, Petsophonsakul P, Halder M, Maresz K, Kramann R and Schurgers L. Vitamin K2 Needs an RDI Separate from Vitamin K1. Nutrients. 2020; 12 (6): Article 1852: 1-13. DOI: 10.3390/nu12061852.
12. Kim TH, Kim HJ, Lee SH and Kim SY. Potent inhibitory effect of Foeniculumvulgare Miller extract on osteoclast differentiation and ovariectomy-induced bone loss. International Journal of Molecular Medicine. 2012; 29 (6): 1053-1059. DOI: 10.3892/ijmm.2012.950.
13. Liu XL, Li CL, Lu WW, Cai WX and Zheng LW. "Skeletal site-specific response to ovariectomy in a rat model: change in bone density and microarchitecture," Clinical Oral Implants Research. 2015; 26 (4):392–398. DOI: 10.1111/clr.12360.

14. Rajfer RA, Flores M, Abraham A, Garcia E, Hinojosa N, Desai M, Artaza JN and Ferrini MG. Prevention of Osteoporosis in the Ovariectomized Rat by Oral Administration of a Nutraceutical Combination That Stimulates Nitric Oxide Production. Hindawi Journal of Osteoporosis. 2019; Volume 2019, Article 1592328: 1-11. DOI: 10.1155/2019/1592328.

15. Merghani BH, Awadin WF, Elseady YY and Abu-Heakal NSA. Protective Role of Wheat Germ Oil against Hyperglycemia and Hyperlipidemia in Streptozotocin Induced Diabetic Rats. Asian Journal of Animal and Veterinary Advances. 2015; 10 (12): 852-864. DOI: 10.3923/ajava.2015.852.864.

16. Gao X, Ma W, Dong H, Yong Z and Su R. Establishing a rapid animal model of osteoporosis with ovariectomy plus low calcium diet in rats. International Journal of Clinical and Experimental Pathology. 2014; 7 (8):5123-5128. PMID: 25197386; PMCID: PMC4152076.

17. Gülle K, Şirin FB, Akpolat M, Öğrenim G, Alkan A and Cesur G. Effects of curcumin and melatonin on bone formation in orthopedically expanded suture in rats: A biochemical, histological and immunohistochemical study. Orthodontics and Craniofacial Research. 2018; 21:160–167. DOI: 10.1111/ocr.12232.

18. Ying X, Chen X, Wang T, Zheng W, Chen L and Xu Y. Possible osteoprotective effects of myricetin in STZ induced diabetic osteoporosis in rats .European Journal of Pharmacology. 2019; 866: Article 172805: 1-24. DOI: 10.1016/j.ejphar.2019.172805.

19. Suvarna KS, Layton C and Bancroft J. Bancroft's theory and practice of histological techniques. 8thed. Elsevier. Amsterdam, Netherland. 2019; pp 114 – 305. https://doi.org/10.1016/C2015-0-00143-5.

20. Sodek J, Ganss B and McKee MD. Osteopontin. Critical Reviews in Oral Biology and Medicine. 2000; 11 (3): 279 303.DOI: 10.1177/10454411000110030101.

21. Zhang B, Sun Y, Chen L, Guan C, Guo L and Qin C. Expression and distribution of SIBLING proteins in the predentin/dentin and mandible of hypmice. Oral Diseases. 2010; 16 (5): 453 464. DOI: 10.1111/j.1601-0825.2010.01656.x.

22. Elkalawy SAE, Abo Gazia MM, Elekhtiar SAAE and Ismail DI. Collagen Hydrolysate Against Fluvoxamine Maleate-Induced Osteoporosis in Albino Rats: A Histological and Immunohistochemical Study. Egyptian journal of Histology. 2020; 43 (4): 988-1007. DOI: 10.21608/EJH.2020.22975.1239.

23. Kasem MA, Khedr EG, Abdel-Aleem AM and Said AS. Histological Effect of Bisphosphonate, Vitamin D and Olive Oil on Glucocorticoid Induced Osteoporosis (Gio) in Albino Rat. The Egyptian Journal of Hospital Medicine. 2016; 65 (1): 699- 708. DOI: 10.12816/0033786.

24. Baloğlu M and Gökalp-Özkorkmaz E. Biochemical and immunohistochemical investigations on bone formation and remodelling in ovariectomised rats with tamoxifen citrate administration. Folia Morphologica. 2019; 78 (4): 789–797. DOI: 10.5603/FM.a2019.0035.

25. Zheng H, Qi S and Chen C. Salidroside Improves Bone Histomorphology and Prevents Bone Loss in Ovariectomized Diabetic Rats by Upregulating the OPG/RANKL Ratio.Molecules. 2018; 23 (9): Article 2398: 1-14. DOI: 10.3390/molecules23092398.

26. Kozakowski J, Gietka-Czernel M, Leszczy´nska D and Majos A. Obesity in menopause-our negligence or an unfortunate inevitability? Prz. Menopauzalny. 2017; 16 (2): 61–65. DOI: 10.5114/pm.2017.68594.

27. Gavin KM, Kohrt WM, Klemm DJ and Melanson EL. Modulation of energy expenditure by estrogens and exercise in women. Exercise and Sport Sciences Reviews. 2018; 46 (4):232-239. DOI: 10.1249/JES.0000000000000160.

28. Lombardo M, Perrone MA, Guseva E, Aulisa G, Padua E, Bellia C, Della-Morte D, Lellamo F, Caprio M and Bellia A. Losing Weight after Menopause with Minimal Aerobic Training and Mediterranean Diet. Nutrients. 2020; 12 (8): Article 2471:1-12. DOI: 10.3390/nu12082471.

29. Maffei S, Forini F, Canale P, Nicolini G and Guiducci L. Gut Microbiota and Sex Hormones: Crosstalking Players in Cardiometabolic and Cardiovascular Disease. International Journal of Molecular Sciences. 2022; 23 (13): Article 7154: 1-21. DOI: 10.3390/ijms23137154.

30. Shakoor S, Ilyas F, Abbas N, Mirza MA and Arif S. Prevalence of osteoporosis in relation to serum calcium and phosphorus in aging women. Journal of Global Innovations in Agricuitural and Social Sciences. 2014; 2 (2): 70-75. DOI: 10.17957/JGIASS/2.2.511.

31. Pardhe BD, Pathak S, Bhetwal A, Ghimire S, Shakya S, Khanal PR and Marahatta SB. Effects of age and estrogen on biochemical markers of bone turnover in postmenopausal women: a population based study from Nepal. International Journal of Women's Health. 2017; 9:781–788. DOI: 10.2147/IJWH.S145191.

32. Gurban CV, Balas MO, Vlad MM, Caraba AE, Jianu AM, Bernad ES, Borza C, Banicioiu-Covei S and Motoc AG. Bone turnover markers in postmenopausal osteoporosis and their correlation with bone mineral density and menopause duration. Romanian Journal of Morphology and Embryology. 2019; 60 (4):1127–1135. PMID: 32239087.

33. Atalay S, Elci A, Kayadibi H, Onder CB and Aka N. Diagnostic utility of osteocalcin, undercarboxylatedosteocalcin, and alkaline phosphatase for osteoporosis in premenopausal and postmenopausal women. Annals of Laboratory Medicine. 2012; 32 (1):23–30. DOI: 10.3343/alm.2012.32.1.23.

34. Chethan KN, Zuber M, Bhat SN, Satish B and Shenoy SB. Comparative Study of Femur Bone Having Different Boundary Conditions and Bone Structure Using Finite Element Method. The Open Biomedical Engineering Journal. 2018; 12: 115-134. DOI: 10.2174/1874120701812010115.

35. Chainy GB and Sahoo DK. : Hormones and oxidative stress: an overview. Free Radical Research. 2020; 54 (1): 1-26. DOI: 10.1080/10715762.2019.1702656.

36. EL-Haroun H, Soliman M, Soliman MA and Abd El Gawad S. Comparative Study on the Possible Protective Effect of LepidiumSativum versus Teriparatide in Induced Osteoporosis in Adult Male Guinea Pigs. Egyptian Journal of Histology. 2020; 43 (3): 931- 947. DOI: 10.21608/EJH.2020.18855.1193.

37. Oršoli´c N, Nemrava J, Jeleˇc Ž, Kukolj M, Odeh D, Jakopovi´c B, Jazvinš´cakJembrek M, Bagatin T, Fureš R and Bagatin D. Antioxidative and Anti-Inflammatory Activities of Chrysin and Naringenin in a Drug-Induced Bone Loss Model in Rats. International Journal of Molecular Science. 2022; 23 (5): Article 2872:1-24. DOI: 10.3390/ijms23052872.

38. Muruganandan S, Ionescu AM and Sinal CJ. At the Crossroads of the Adipocyte and Osteoclast Differentiation Programs: Future Therapeutic Perspectives. International Journal of Molecular Science. 2020; 21(7): Article 2277: 1-15. DOI: 10.3390/ijms21072277.

39. Kalleny N. Histological and morphometric studies on the effect of alphalipoic acid on postovariectomy osteoporosis induced in adult female albino rats. Egyptian Journal of Histology. 2011; 34 (1):139–155. DOI: 10.1097/01.EHX.0000395006.52039.6c.

40. Sharaf HA, Shaffie NM, Morsy FA, Badawi MA and Abbas NF. Role of some phytoestrogens in recovering bone loss: histological results from experimental ovariectomized rat models. Journal of the Arab Society for Medical Research. 2015; 10 (2):65–75. DOI: 10.4103/1687-4293.175880.

41. Liu Z, Liu L, Kang C, Xie Q, Zhang B and Li Y. Effects of estrogen deficiency on microstructural changes in rat alveolar bone proper and periodontal ligament. Molecular Medicine Reports. 2015; 12 (3): 3508-3514. DOI: 10.3892/mmr.2015.3891.

42. Chen C, Zheng H and Qi S. Genistein and silicon synergistically protects against ovariectomy-induced bone loss through upregulating OPG/RANKL ratio. Biological Trace Element Research. 2019; 188 (2): 441-450. DOI: 10.1007/s12011-018-1433-8.

43. Rajan R, Paul J, Kapoor N, Cherian KE and Paul TV. Postmenopausal osteoporosis – An Indian perspective. Current Medical Issues. 2020; 18 (2): 98-104. DOI: 10.4103/cmi.cmi_5_20.

44. Abd El Fattah ER, Abd El Fattah MT and EL-Bestawy EM. Possible Protective Role of L-Carnitine Against Hyperthyroidism Induced Osteoporotic Changes In Femoral Diaphysis of Adult Male Albino Rats. Egyptian journal of Histology. 2023; 46 (1): 91-104. DOI: 10.21608/EJH.2021.86696.1528.

45. Vancea A, Serban O and Fodor D. Relationship between Osteopontin and Bone Mineral Density. Acta Endocrinol (Buchar). 2021; 17(4):509-516. DOI: 10.4183/aeb.2021.509.

46. Dos Santos EA, Giudici KV, de France NA, Peters BS, Fisberg RM and Martini LA. Is the dietary intake of vitamin K associated with obesity parameters among adolescents? Demetra: Food, Nutrition & Health. 2019; 14 (9): 1-16. DOI: 10.12957/demetra.2019.39079.

47. Knapen MH, Schurgers LJ, Shearer MJ, Newman P, Theuwissen E and Vermeer C. Association of vitamin K status with adiponectin and body composition in healthy subjects: uncarboxylatedosteocalcin is not associated with fat mass and body weight. British journal of nutrition. 2012; 108 (6): 1017-1024. DOI: 10.1017/S000711451100626X.

48. Elghazaly NA, Radwan EH, Hala H, Zaatout HH, Elghazaly MM and Allam NE. Beneficial Effects of Fennel (FoeniculumVulgare) in Treating Obesity in Rats. Journal of Obesity Management. 2019; 1 (2): 16-33. DOI: 10.14302/issn.2574-450X.jom-18-2484.

49. Noreen S, Tufail T, Tufail T, Bader Ul, Ain H, Jaffar HM, Awuchi CG. Cookies enriched with anethole and secoisolariciresinol diglucoside from flaxseed and fennel seeds improve hypercholesterolemia, lipid profile, and liver functions: A pilot study. Food Sci Nutr. 2023; 15; 11(7):4211-4218. DOI: 10.1002/fsn3.3433.

50. Bellido T and Plotiken LI. Novel action of bisphosphonates in bone: preservation of osteoblast and osteocyte viability. Bone. 2011; 49 (1): 50- 55. DOI: 10.1016/j.bone.2010.08.008.

51. Simes DC, Viegas CS, Araújo N and Marreiros C. Vitamin K as a Diet Supplement with Impact in Human Health: Current Evidence in Age-Related Diseases. Nutrients. 2020; 12 (1): Article 138:1-24. DOI: 10.3390/nu12010138.

52. Ma X, Xu Z, Ding S, Yi G and Wang Q. Alendronate promotes osteoblast differentiation and bone formation in ovariectomy induced osteoporosis through interferon β/signal transducer and activator of transcription 1 pathway. Experimental and Therapeutic Medicine. 2018; 15 (1): 182-190. DOI: 10.3892/etm.2017.5381.

53. Ukon Y, Makino T, Kodama J, Tsukazaki H, Tateiwa D, Yoshikawa H and Kaito T. Molecular-Based Treatment Strategies for Osteoporosis. International Journal of Molecular Sciences. 2019; 20 (10): Article 2557: 1-24. DOI: 10.3390/ijms20102557.

54. 54- Rishavy MA and Berkner KL. Vitamin K oxygenation, glutamate carboxylation, and processivity: defining the three critical facets of catalysis by the vitamin K-dependent carboxylase. Advances in Nutrition. 2012; 3 (2): 135–148. DOI: 10.3945/an.111.001719.

55. 55- Haugsgjerd TR, Egeland GM, Nygård OK, Vinknes KJ, Sulo G, Lysne V, Igland G and Tell GS. Association of dietary vitamin K and risk of coronary heart disease in middle-age adults: the Hordaland Health Study Cohort. BMJ Open. 2020; 10(5): Article e035953: 1-11. DOI: 10.1136/bmjopen-2019-035953.

الملخص العربى

دراسة نسيجية وهستوكيميائية مناعية وقياسيه بينيه على التأثير العلاجي المحتمل لكل من حمض أليندرونيك (فوساماكس) / وفيتامين (ك٢) والشمر منفردين ومجتمعين على هشاشة العظام الناجم عن استئصال المبايض فى الجرذان

هبه يوسف اليماني ابو دغيد ، حكمت احمد سرور، منى محمد عبد الجليل السيد

قسم الهستولوجيا وبيولوجيا الخلية - كلية الطب (بنات)-جامعة الازهر

المقدمة: يمثل هشاشة العظام بعد انقطاع الطمث اضطرابًا استقلابيًا في العظام في جميع أنحاء العالم بسبب انخفاض مستويات الأستروجين بشكل كبير ، وانخفاض القدرة على الاستفادة من الكالسيوم وانخفاض إمدادات فيتامين د.

الهدف من البحث: تقييم دور حمض أليندرونيك (فوساماكس) وفيتامين (ك٢)/ و زيت الشمر العطري في تحسين مرض هشاشة العظام الناجم عن استئصال المبايض في اناث الجرذان البيضاء البالغة.

المواد والطرق: تم اجراء هذا البحث على ثمانية وأربعون جرذا من اناث الجرذان البيضاء البالغة التي تزن١٨٠ ± ٢٠جرام وتتروح اعمارهن بين١٢ إلى ١٤ أسبوعا وتم تقسيمهم إلى المجموعات الاتية:

المجموعة الأولى: المجموعة الضابطة.

المجموعة الثانية : تعرضت لإخراج المبايض من مكانها دون إزالتها ثم اعيدت الى موضعها بالجسم جراحيا.

المجموعة الثالثة (مجموعة استئصال المبايض): تم اسئصال المبايض جراحيا من ثلاثون جرذا من اناث الجرذان البيضاء البالغة. بعد مرور اثنى عشر أسبوعا من جراحة استئصال المبايض تم تقسيم جرذان هذه المجموعة بالتساوى الى خمس مجموعات فرعية وهذه المجموعات هي:

- المجموعة الثالثة أ (مجموعة هشاشة العظام):تركت جرذان هذه المجموعة دون أي تدخل علاجى لمدة ١٢ أسبوعًا.
- المجموعة الثالثة ب (مجموعة هشاشة العظام المعالجة بالفوزاماكس): تلقت جرذان هذه المجموعة ١مل من محلول الفوزاماكس بجرعة مقدارها ٢,٠ مجم/ مل/جرذ اسبوعيا.
- المجموعة الثالثة ج (مجموعة هشاشة العظام المعالجة بالمينا كيو): هذه المجموعة اعطيت ١ مل من محلول مينا كيو بجرعة تعادل ٥,٠ مجم / مل/جرذ يوميا.
- المجموعة الثالثة د (مجموعة هشاشة العظام المعالجة بزيت الشمر): هذه المجموعة اعطيت يوميا ا مل من زيت الشمر.
- المجموعة الثالثة ه (مجموعة هشاشة العظام المعالجة بكل من المينا كيو وزيت الشمر): تلقت جرذان هذه المجموعة محلول مينا كيو قبل اعطاء زيت الشمر بساعة واحدة بنفس الجرعات ولنفس المدة المقررة كما في المجموعتين الثالثة ج و الثالثة د على الترتيب.

أعطيت جميع العلاجات السابقة للجرذان بواسطة أنبوب معدى على مدار ١٢ أسبوع.

تم فصل مصل الدم للاختبارات المعملية. كما تم تحضير عينات من عظم الفخذ لفحصها نسيجيا. كما تم اجراء التحليلات القياسيه البينيه والاحصائية لكافة النتائج.

النتائج: احتوت مجموعة هشاشة العظام على مناطق بؤرية غير متجانسة في مصفوفة العظام ظهرت مصبوغة بشكل باهت مع مناطق قاعدية زرقاء غير منتظمة بينهما. كما ظهرت تجاويف هشاشة العظام ، أنفاق كبيرة ، مناطق خالية من الخلايا العظمية ، وعدد قليل من الثغرات الفارغة. وقد كشفت البطانة الداخلية لعظم الفخذ عن سطح متآكل بشكل غير متساوي. تم دعم هذه النتائج من خلال انخفاض كبير في مستويات الكالسيوم والفوسفور في السيوم مقرونًا بزيادة كبيرة في مستويات إنزيمات الفوسفاتيز القلوية الخاصة بالعظام (BALP) وفوسفاتاز حمض الطرطرات المقاوم (TRAP) وانخفاض كبير في النسبة المئوية لمساحة ألياف الكولاجين وفي تفاعل شيف داخل مصفوفة العظام. كما كشفت الدراسات الهستوكيميائية المناعية عن تعبير مناعي إيجابي لـمنشط مستقبلات العامل النووي RANKL في تجاويف هشاشة العظام ونشاط مناعي ضعيف لبروتين الاستيوبونتين Osteopontin في مصفوفة العظام. بينما أظهر فوساماكس وفيتامين ك٢ وزيت الشمر العطري تحسنًا ملحوظًا في التغيرات النسيجية التي تم وصفها سابقًا.

خلاصة البحث: كان الجمع بين مركبات زيت الشمر العطري و المينا كيو أكثر فعالية في تعزيز علاج مرض هشاشة العظام بعد انقطاع الطمث بخلاف اى من المينا كيو ، أو الشمر منفردا أو بعقار فوساماكس. وقد يعزى ذلك إلى الخصائص المضادة للأكسدة والمضادة للالتهابات لكل من المينا كيو ، و الشمر بالإضافة إلى التأثيرالاستروجيني القوي للشمر.